Educational Hardware for Feedback Systems

by

Isaac Dancy

Submitted to the Department of Electrical Engineering and Computer Science
in partial fulfillment of the requirements for the degree of

Master of Engineering in Electrical Engineering and Computer Science

at the

MASSACHUSETTS INSTITUTE OF TECHNOLOGY

September 2004

Author .....
Department of Electrical Engineering and Computer Science
September 8, 2004

Certified by .....
Dr. Kent Lundberg
Post-Doctoral Lecturer
Thesis Supervisor

Accepted by .....
Arthur C. Smith
Chairman, Department Committee on Graduate Students

Educational Hardware for Feedback Systems

by

Isaac Dancy

Submitted to the Department of Electrical Engineering and Computer Science
on September 8, 2004, in partial fulfillment of the
requirements for the degree of
Master of Engineering in Electrical Engineering and Computer Science

Abstract

This thesis explores a variety of educational feedback systems with an emphasis on developing them for in-class demonstrations and in-depth student projects. The nature of feedback systems means there is never a shortage of demonstrations or assignments that can truly capture the students' imagination and enthusiasm for class material. Unfortunately, it is sometimes the case that the feedback systems with the most potential for greatness are also unreliable, inaccurate, and inconsistent.

This thesis attempts to narrow the gap by exploring, analyzing, and building a variety of exciting feedback systems. A comparison of general-purpose and high-performance operational amplifiers is created. Hardware for a web-based laboratory on canonical second-order systems is implemented. Cheap magnetic levitation kits for in-term projects are made even cheaper. And finally, the inverted pendulum — a decades-old Course VI heirloom and featured demonstration — is restored to its past glory.

Thesis Supervisor: Dr. Kent Lundberg
Title: Post-Doctoral Lecturer

Acknowledgments

A special thanks to Marita, Jacob, Zoë, Leah, Ada, Mira, Anthony, Jesse, Leigh, Abram, Mike and Cora. You never do see it written in that order. I'll leave the second generation of Dancy names for the next thesis acknowledgement.

I would also like to acknowledge those in the the field who inspire a passion for electrical engineering, including Ron Roscoe, Professor J. K. Roberge and those savvy SynQor engineers. Additionally, I could have never completed this project without the unconditional support and assistance of my advisor, Dr. Kent Lundberg.

Thanks to my parents for always pushing me to do my very honest best, even if I still won't smile for a post-strikeout photo-op.

And of course I need to thank Jenna soon-to-be-Dancy, who handled my thesis burden in her typically beautiful and graceful way.

Contents

Chapter 1

Externally Compensated Operational Amplifier System

1.1 Introduction

Many commercial operational amplifiers are compensated such that they will be stable regardless of what may be connected to their terminals. This conservative compensation approach — while certainly attractive to a wide range of users and pleasing to datasheet appearances — can lead to disappointing performance in many standard applications. Operational amplifiers designed for advanced users and specific applications can outperform general-purpose amplifiers whose goal is simply to work, but not to work well.

The OP27 and OP37 operational amplifiers by Analog Devices provide an excellent demonstration of this situation [1, 2]. The OP27 is a general-purpose amplifier with pleasing all-around specifications and guaranteed stability for all gain configurations below its own open-loop gain. The OP37 is a similar product, but has been optimized for applications with gains greater than five and cannot guarantee the same stability as the OP27 for gains below five. The datasheets, however, reveal that the OP37 slews at a rate of 17 V/μs, while the OP27 slews nearly an order of magnitude behind at a very quaint and unimpressive 2.8 V/μs.

The OP37 dominantly outperforms the OP27, even within a related product line

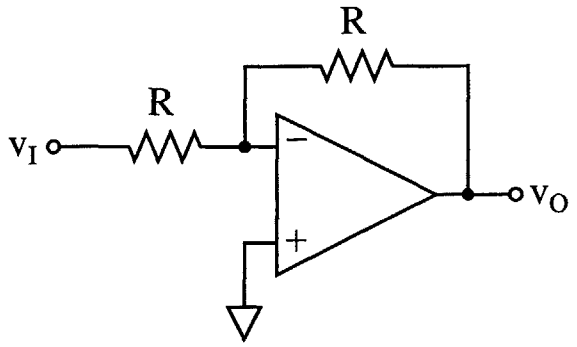

Figure 1-1: Inverting-gain-of-1 amplifier.

and device family, because it is optimized for high slew rates and bandwidth, thereby sacrificing stability at lower closed-loop gains. This optimization means that the OP27 and the OP37 are not completely compatible in common circuit configurations. If a user replaced an OP27 in an inverting-gain-of-two amplifier with an OP37, the circuit will no longer operate correctly, and this observation is often to the surprise and bewilderment of the user making the change.

The OP37, however, really *could* work if the external system was designed properly.

The motivation driving an opamp demonstration for feedback systems is to show how higher-performance parts can be used in applications where at first glance they appear to fail. Circuit designers with a broad knowledge of classical feedback can use simple, external compensation to fix the problems present in the unstable feedback loop. This demonstration will juxtapose two inverting followers; one circuit using the pedestrian OP27, and another externally compensated configuration using the much faster OP37. The increased transient performance of the OP37 will be striking, while stressing to students the not-so-subtle fact that careful measures are absolutely required to ensure stability.

1.2 Analysis

This demonstration focuses on the inverting-gain-of-1 circuit, shown in Figure 1-1. To better understand the stability dynamics, the analysis must ignore the usual ideality approach taught in many introductory courses.

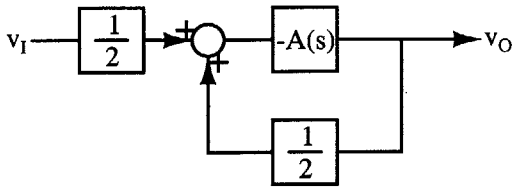

Figure 1-2: Inverting-gain-of-1 block diagram.

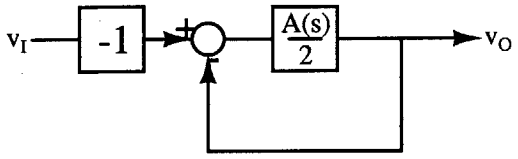

Figure 1-3: Inverting-gain-of-1 unity-feedback block diagram.

Figure 1-2 illustrates the block diagram for this circuit and Figure 1-3 is the simplified, unity-feedback block diagram for the same system. Basic block diagram manipulation provides the simplification between Figures 1-2 and 1-3; that is, when pushing a multiplicative factor through a summing junction, the reciprocal appears at the output. Note in Figure 1-3 that the ideal input-output relation preceeds the feedback loop while the loop represents some dynamics with a final value of one. Another equally important (though often neglected) point is the fact that this amplifier reduces the loop gain by a factor of one-half, which seems nonintuitive for a closed-loop unity-gain amplifier. Alas, the gain-bandwidth product is deceiving in this application.

Nevertheless, a simple Bode analysis should be sufficient to predict the closed-loop behavior of the system. The advantage of a Bode analysis is that only the open-loop behavior is considered, thus avoiding any extraneous math where additional errors can occur. The open-loop frequency response of the augmented loop transmission is all that is required for a Bode analysis.

The phase margin of the OP27 circuit at the crossover frequency of $A(s)/2$ is approximately 90° at 5 MHz, as indicated by the OP27 datasheet and reproduced in Figure 1-4. With an OP37, however, the phase margin at crossover is either close to zero or nonexistent — the datasheet doesn't even reveal the phase at this open-loop location. This omission is to be expected since Analog Devices do not guarantee

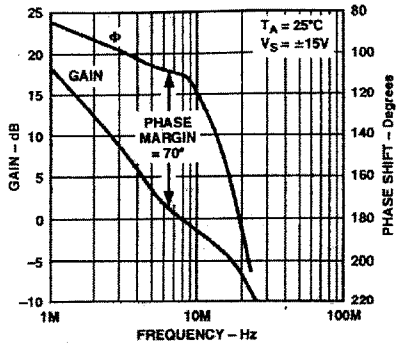

TPC 18. Gain, Phase Shift vs. Frequency

Figure 1-4: OP27 open-loop frequency-response characteristic, as it appears in [1].

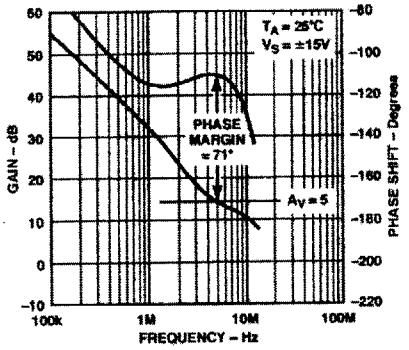

TPC 18. Gain, Phase Shift vs. Frequency

Figure 1-5: OP37 open-loop frequency-response characteristic, as it appears in [2].

stability for closed-loop gains less than five, let alone 1.

Thus, the challenge put forth in this demonstration is to design an inverting-gain-of-1 amplifier using a single OP37 by reducing its loop gain by at least a factor of five, ensuring a large positive phase margin, and consequently, superior transient characteristic when compared to the OP27.

1.3 Design

1.3.1 Reduced-Gain Compensation

The OP37's problem is that its loop gain is greater than one when the phase drops rapidly. Closed-loop systems calling for higher gain will invariably have a loop trans-

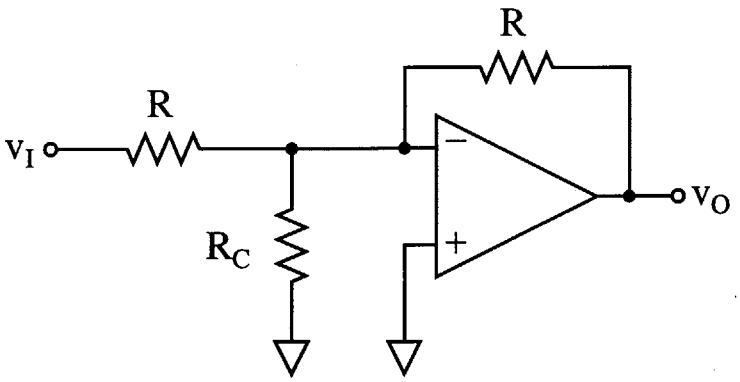

Figure 1-6: Reduced-gain amplifier configuration.

mission with less gain, meaning that stability is not a problem. A reduction of loop transmission can still be achieved without effecting closed-loop gain by adding a resistance at the inverting terminal of the operational amplifier. Figure 1-6 illustrates this configuration, implementing a form of *reduced-gain* compensation.

To develop the block diagram describing this configuration, it is necessary to solve for the voltage at the inverting input of the op amp. Superposition of v_I and v_O yields

$$v_- = \frac{R||R_C}{R + R||R_C} v_I + \frac{R||R_C}{R + R||R_C} v_O, \tag{1.1}$$

while the open-loop characteristic of the op amp determines

$$v_O = -A(s)v_-. \tag{1.2}$$

These relations combine to develop a block diagram description of the amplifier (Figure 1-7). Block diagram manipulation simplifies Figure 1-7 into the unity-feedback configuration, shown in Figure 1-8. The ideal relation of this configuration is still a gain of -1, yet the loop gain has become

$$L(s) = \frac{R||R_C}{R + R||R_C} A(s). \tag{1.3}$$

Therefore, if the quantity $R||R_C/(R + R||R_C)$ is less than or equal to $\frac{1}{5}$, then the system has achieved at least 70° of phase margin while matching the low gain of the OP27. The value of compensation resistor to ensure stability is

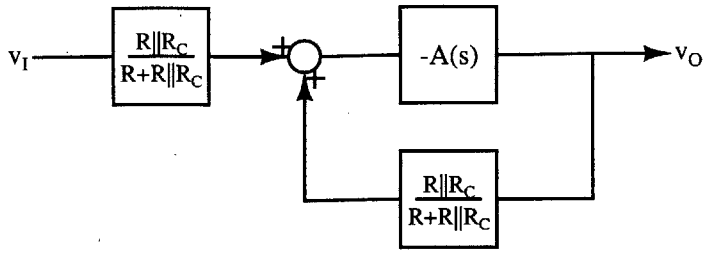

Figure 1-7: Reduced-gain amplifier block diagram.

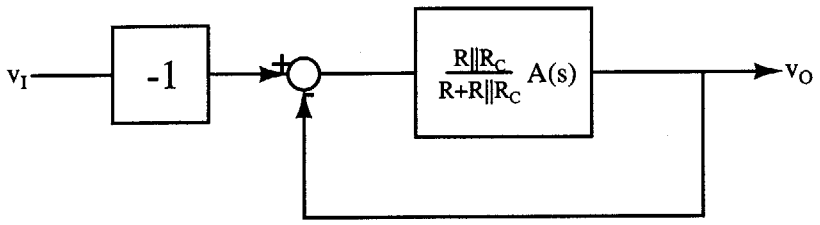

Figure 1-8: Reduced-gain, unity-feedback amplifier block diagram.

$$R_C \leq \frac{1}{3}R. \tag{1.4}$$

The reduced-gain compensation was implemented in this demonstration with $R =$ 10 kΩ and $R_C = 1.3$ kΩ, a reduced-gain compensation of 0.103.

1.3.2 Lag Compensation

One disadvantage of the compensation technique described in the previous section is the fact that it reduces the gain of the loop transmission over all frequencies, when it is only necessary near the crossover frequency. Reduced-gain compensation unnecessarily decreases the DC gain of the open-loop, and thus degrades the steady-state error response of the closed-loop response. Lag compensation can replace reduced-gain compensation to maintain open-loop low frequency gain while also ensuring a safe crossover phase margin.

Lag compensation can be realized with a series R_{lag}-C circuit applied instead of the reduced-gain resistor, R_C (shown in Figure 1-9). The impedance of the lag branch is

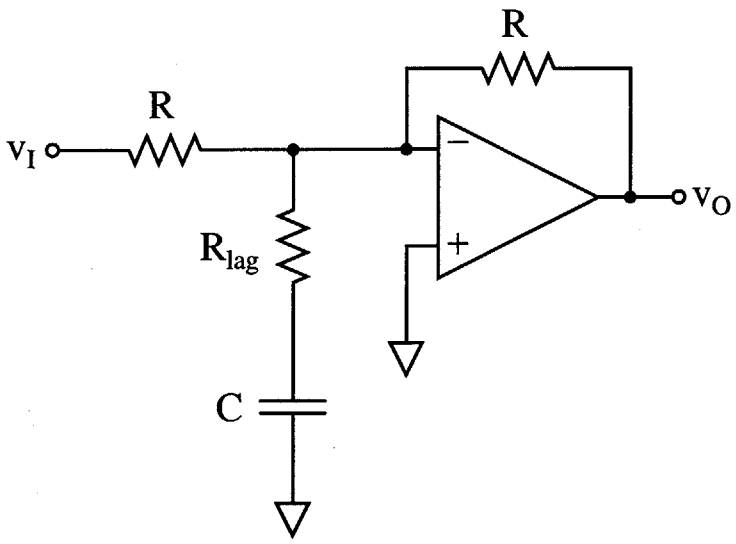

Figure 1-9: Lag compensation configuration.

$$Z_C(s) = \frac{R_{\text{lag}}Cs + 1}{Cs}. \tag{1.5}$$

To understand how the lag compensation will behave, simply substitute $Z_C(s)$ for R_C in the reduced-gain equation. This substitution into Equation 1.3 yields the loop gain characteristic for the lag-compensated configuration

$$L(s) = \frac{1}{2}\frac{(R_{\text{lag}}Cs + 1)}{(\frac{R}{2} + R_{\text{lag}})Cs + 1}A(s). \tag{1.6}$$

This implementation of lag compensation is not perfect, as there is still a one-half reduction of DC gain, but this fraction is still a vast improvement over the previous reduced-gain compensation of 0.103.

This lag compensation was implemented with $R = 10\ \text{k}\Omega$, $R_{\text{lag}} = 560\ \Omega$, and $C = 259$ pF.

1.4 Results

The OP27 inverting-gain-of-1 circuit was built as well as a selectable reduced-gain, lag-compensated circuit built with an OP37. Both circuits were driven by a ring oscillator circuit which transitions faster than either opamp could possibly match,

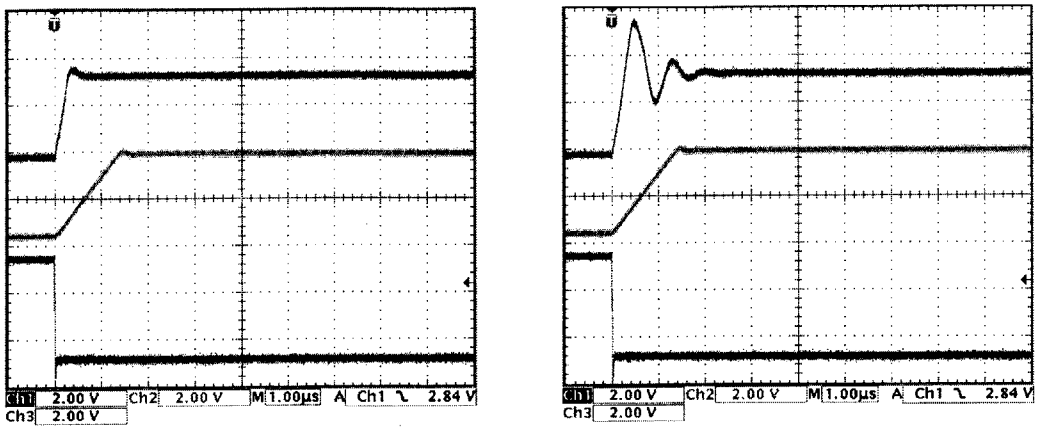

(*a*) OP27 versus reduced-gain OP37. (*b*) OP27 versus lag-compensated OP37.

Figure 1-10: Measured Results. Top trace is the OP37 response, middle trace is the OP27 response, and the bottom trace is the ring oscillator drive signal.

thus ensuring that both circuits will slew. A complete schematic can be found in Figure 1-11.

A comparison of the OP27 to the reduced-gain OP37 circuit is shown in Figure 1-10*a*, and a comparision with the lag-compensated OP37 follows in Figure 1-10*b*. It is clear in both cases that the OP37 configuration slews faster.

1.5 Future Work

While the demonstration convincingly illustrates the difference in slew rate between the OP27 and OP37, it would also be preferable that there be some way to illustrate the difference in steady-state error between the reduced-gain and lag compensation configurations. The error is expressed in the voltage present at the inverting terminal of the op amp, but unfortunately this voltage is too small to detect. This demonstration would be enhanced if some means to display the error voltage of the OP37 were possible.

Furthermore, the response of the lag compensated response (Figure 1-10*b*) suggests less open-loop phase margin than the corresponding reduced-gain response. The demo would be improved with a slight adjustment to the compensator such that a greater phase margin was achieved.

1.6 Conclusion

While it is often the goal of operational amplifier manufacturers to produce perfectly stable designs for any user application, this objective is clearly at the sacrifice of better transient behavior. With careful attention to detail, however, many discrete circuit designers can use higher-performance operational amplifiers for a wide range of applications, even if at first glance it appears they would not work.

If it does not work the first time, feedback makes it possible to try, try again.

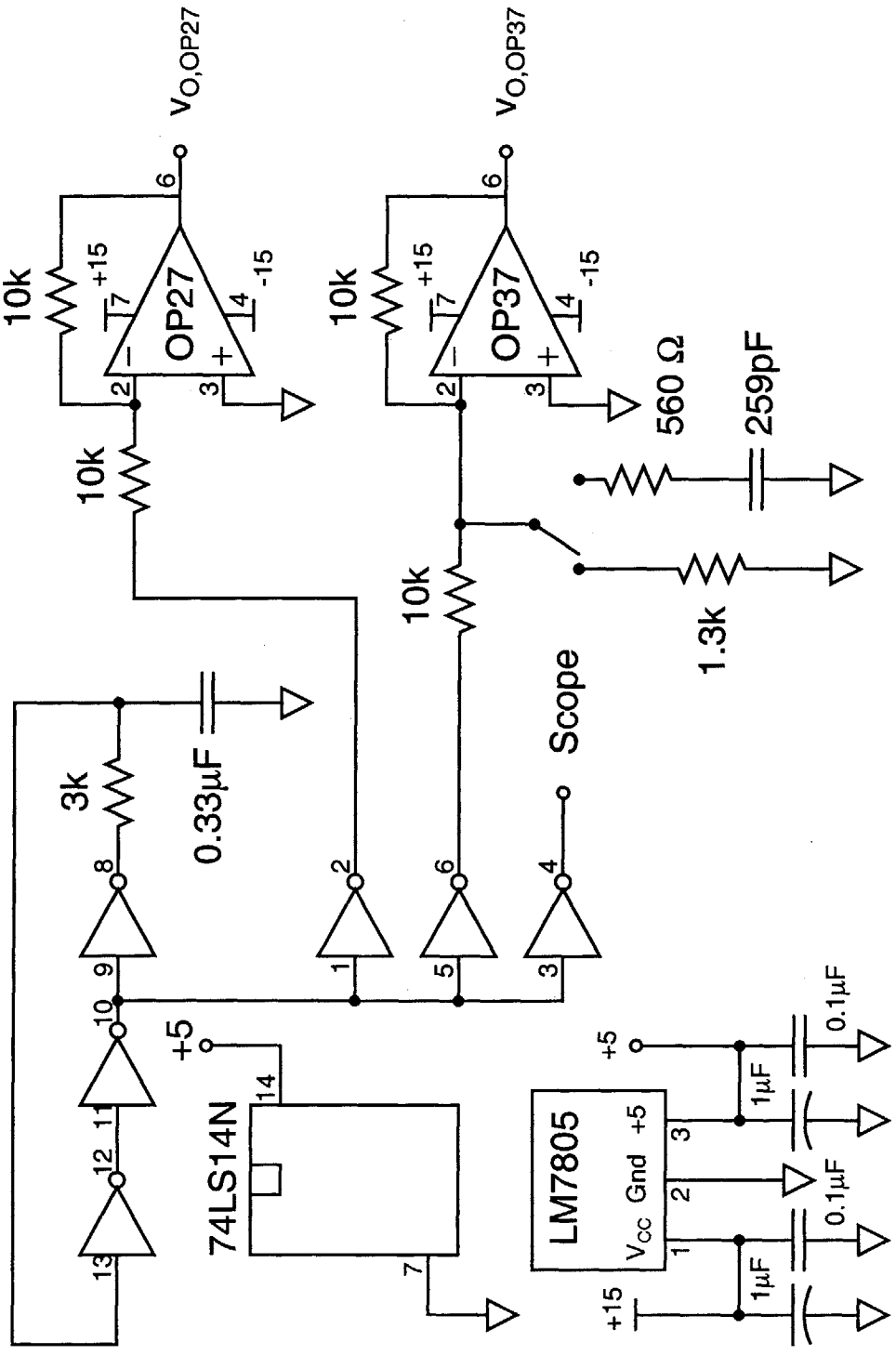

Figure 1-11: Final OP27/OP37 demonstration circuit. 74LS14N implements the ring-oscillated drive signal. Three-position switch selects between lag- and reduced-gain compensation.

Chapter 2

Web-Based Second-Order Systems Laboratory

2.1 Introduction

The first order of semesterly business in many feedback courses is to re-awaken the students' familiarities with basic transfer functions and their behavior. This review is usually achieved with a barrage of pole-zero, step response, or Bode plot associations in homework and a merciless rehashing of terms and definitions in lectures or recitations — or both.

The motivation behind a web-based laboratory on second-order systems is to bypass the prominence and inherent boredom of these expository details and give students an interactive and engaging way to review material while simultaneously providing feedback to course staff with each students' individual degree of understanding of reviewed material.

A "weblab" is a perfect way to achieve this. Weblabs consist of some software front-end running experiments on one back-end device [3]. A weblab designed to test and familiarize students with canonical second-order systems can help to quickly ready students with the more complicated and interesting matters at hand.

With a software interface already in place, all that remains is to build a set of hardware to communicate through the interface and accurately simulate the conditions

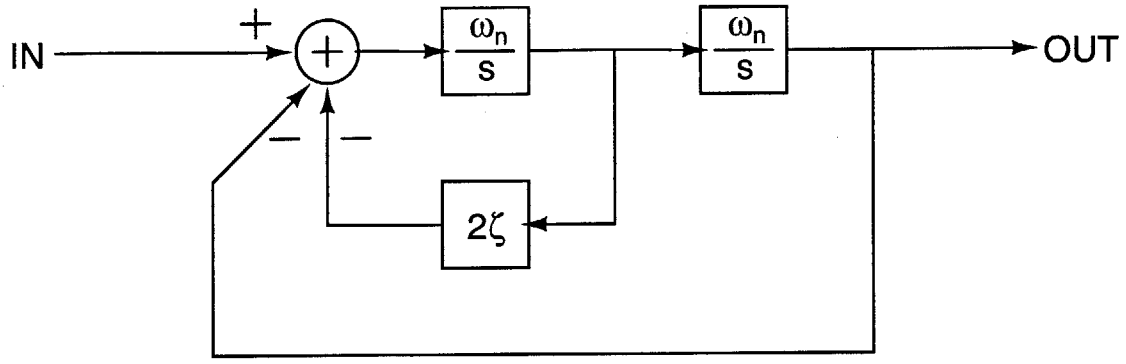

Figure 2-1: State-variable filter topology. Closed-loop transfer function implements the canonical second-order system, using only open-loop integrators and gain elements.

under test [3, 4].

2.2 Analysis

This weblab requires hardware that implements a variety of second-order systems, from lightly damped conjugate pole pairs to over-damped, negative-real-axis poles. The parameters of these systems must also be user-settable via the lab server. To achieve a greater range of systems and results, two canonical second-order systems will be cascaded, giving the user four exclusive degrees of freedom.

The experiment hardware must be either current- or voltage-controlled in order to translate lab server commands into second-order system parameters. The state-variable filter (block diagram shown in Figure 2-1) is a system which can provide such functionality. The basis of the state-variable filter is its dependence on feedback and simple building blocks such as integrators and gain elements.

The closed form of the state-variable filter is

$$H(s) = \frac{\omega_n^2}{s^2 + 2\zeta\omega_n s + \omega_n^2}, \tag{2.1}$$

which is exactly the canonical second-order transfer function. If parameters ω_n and ζ are voltage-controlled, then this topology can implement any second-order frequency

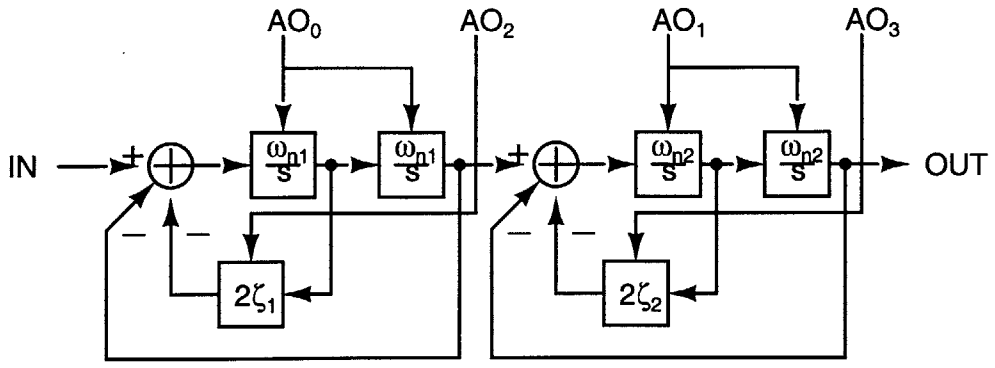

Figure 2-2: Controlled and cascaded state-variable filter system. AO_n signals control the gain of connected system blocks. Cascade provides four user-settable system poles.

response. In fact, this topology is widely used in musical applications due to its broad synthesis capabilities [5, 6].

Thus, the state-variable filter uses simple integrators, gain elements, and feedback to implement a variety of second-order reponses. If the integrator and feedback gains are carefully controlled, then any desired response can be realized. Figure 2-2 represents the overall topology of this cascaded state-variable filter design. AO_n are command signals expressed via the lab server through the hardware interface. A frequency analyzer controls `IN` and measures the response at `OUT`.

2.3 Hardware Interface

The lab server exists on location with the experiment hardware and communicates with the lab broker to receive all client experiment parameters [7]. The LabJack™ connects to the lab server through the universal serial bus (USB) and expresses the client commands for use by the experiment-specific hardware [8].

The LabJack™ drives two analog, 5-volt voltage signals and 20 lines of 5V TTL-compatible digital logic. These 20 lines are programmed into two 10-bit binary signals in the software, yielding a total of four command signals.

The digital signals require some processing before any voltage-controlled exper-

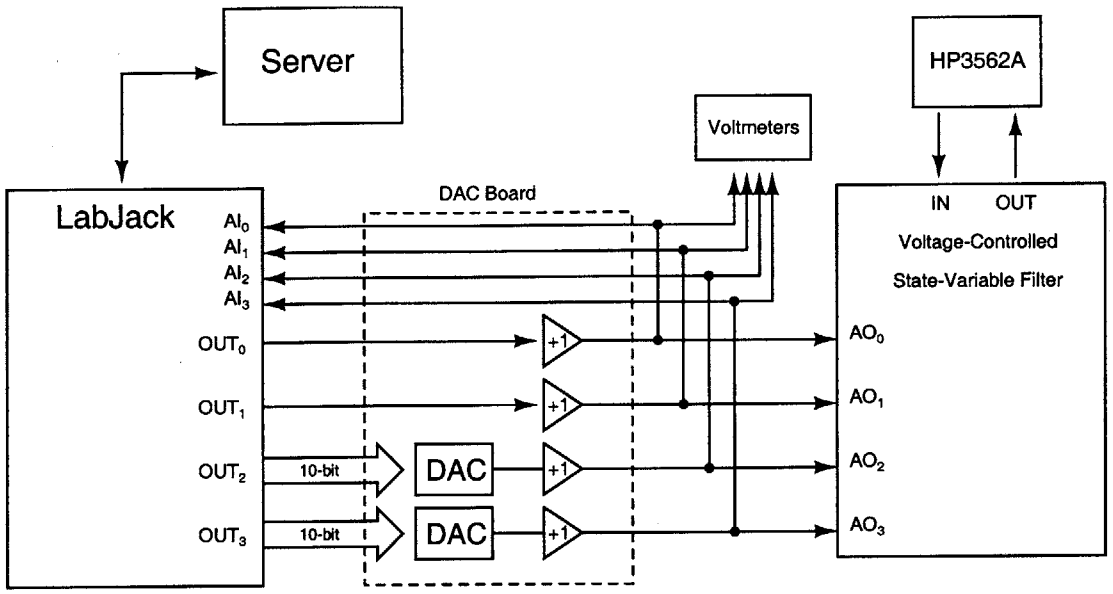

Figure 2-3: Server-side hardware configuration. Voltmeters provide administrators with the current command signals. Lab server controls the HP3562A measurement via the HPIB interface.

iment circuit can possibly make use of them. The processing is performed with separate hardware, which converts the two 10-bit digital command signals into 5-volt analog voltages. An overall diagram of the experiment setup is shown in Figure 2-3.

2.4 Design

The convenience of the state-variable filter design is the reliance on simple variable-gain function elements. The circuit design can focus simply on a variable-gain integrator and implement the feedback topology with simple adder circuits and variable-gain blocks.

2.4.1 Voltage-Controlled Integrator

Often times transimpedance amplifiers form the basis of a variable-gain integrator when current is the command medium [9]. This topology, while correct, performs no better than the linearity of the transimpedance amplifier which implements it, and this specification can often times be limited.

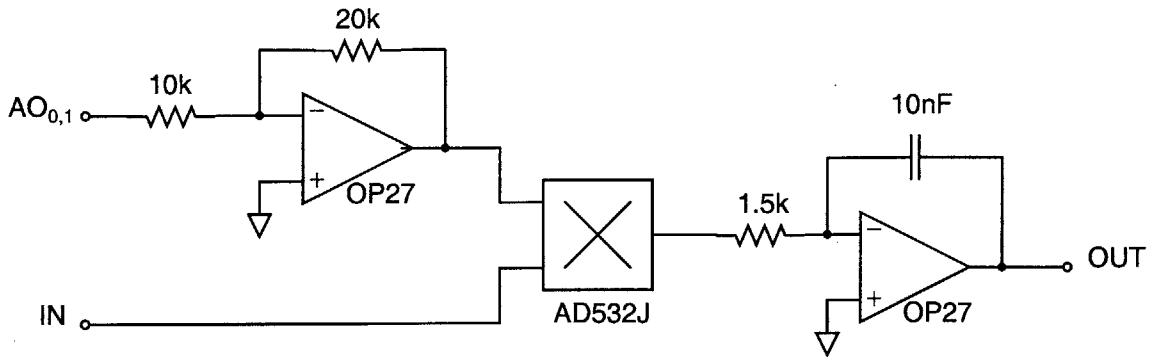

Figure 2-4: Voltage-controlled inverting integrator. Inverting-gain-of-2 amplifier scales $AO_{0,1}$ up to the full range of the AD532J and results in a total noninverting relation from `IN` to `OUT`.

Alternatively, a voltage command signal requires voltage multipliers and instead depends greatly on the linearity of voltage multipliers. Voltage multipliers with greater linearity can be found, though at a price exceeding $29 per chip [10]. Fortunately, Analog Devices generously donated the AD532 voltage multipliers used in this hardware, allowing the design to forego cost and proceed.

The circuit diagram for an inverting integrator is shown in Figure 2-4. The input-output relation for this circuit is

$$\frac{v_O}{v_I} = \left(\frac{v_C}{10\text{ V}}\right)\frac{1}{RCs}, \tag{2.2}$$

where the voltage v_C can be tuned to control the gain of the integrator.

2.4.2 Voltage-Controlled Gain Element

A voltage-controlled gain element can be implemented using another AD532 device, where $v_C/10$ V is the variable-gain parameter.

2.4.3 Final Circuit

These two simple building blocks are configured in the feedback topology to realize the state-variable filter. Two systems are cascaded together to realize a greater variety of systems and assignment possibilities. The 5-volt analog signals are multiplied by

two in order to utilize the full dynamic range of the AD532 chips. The two voltages controlling the ω_n parameters are also inverted to make the integrators noninverting in the open-loop. A final circuit schematic of the state-variable filter is illustrated in Figure 2-5. The complete system consists of two copies of this circuit.

2.5 Results

The total system was built and connected [11]. The system succeeds in producing smooth, accurate frequency responses and compares favorably to theoretical results. Figure 2-6 compares an experimental result to a theoretical result, and confirms this system's functionality.

Additionally, a laboratory assignment (Appendix A) has been written that actively engages students in a productive discovery or review of second-order system responses and parameters. Another assignment, while not based on the weblab itself, does serve to complement the laboratory and can be found in Appendix B.

Students will be expected to evaluate the state-variable filter topology in block diagram and circuit form, finding relations between the voltage command signals and the corresponding block diagram parameters. Students will then relate a sampling of second-order systems (Figures 2-7*a* and 2-7*b*), express these systems in order of their second-order parameters, then calculate the voltages required to make the experiment implement the systems.

While we hope that students will fine-tune their understanding of second-order systems, we also hope that they will make a few observations relating to the limitations of this specific design and implementation — problems inherent in any undertaking of this kind. For example, students should observe the difficulty in simulating the sharp and large-valued gains evident in low-damped systems. Students should also observe the difficulty in discerning between similar systems — i.e., four distinct, negative poles closely clustered versus four poles at one, single location.

Ultimately, students will rediscover and explore second-order systems while realizing the minor issues inherent in the hardware's implementation.

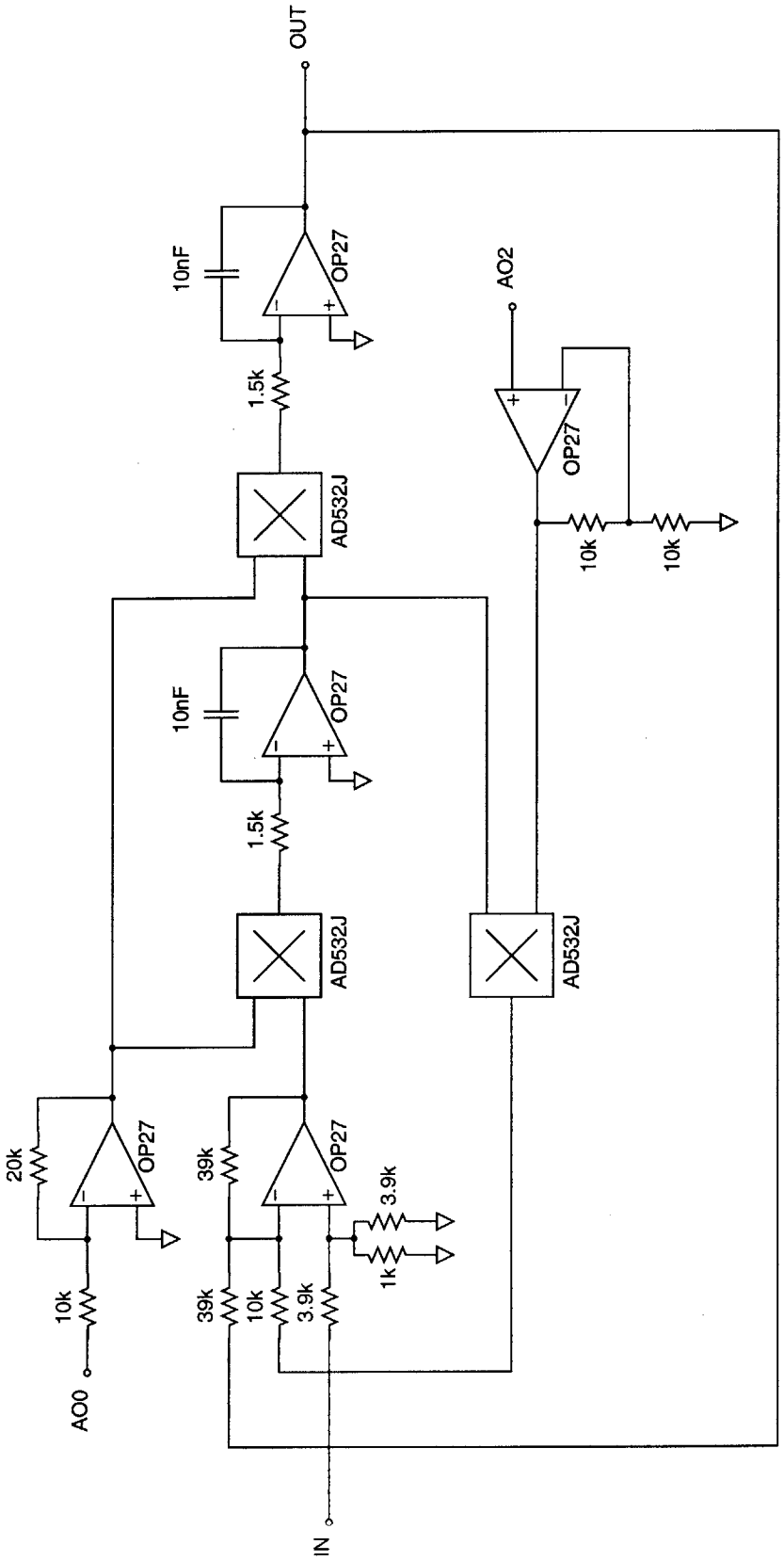

Figure 2-5: State-variable filter circuit implementation. Three multipliers per filter make this circuit expensive to build.

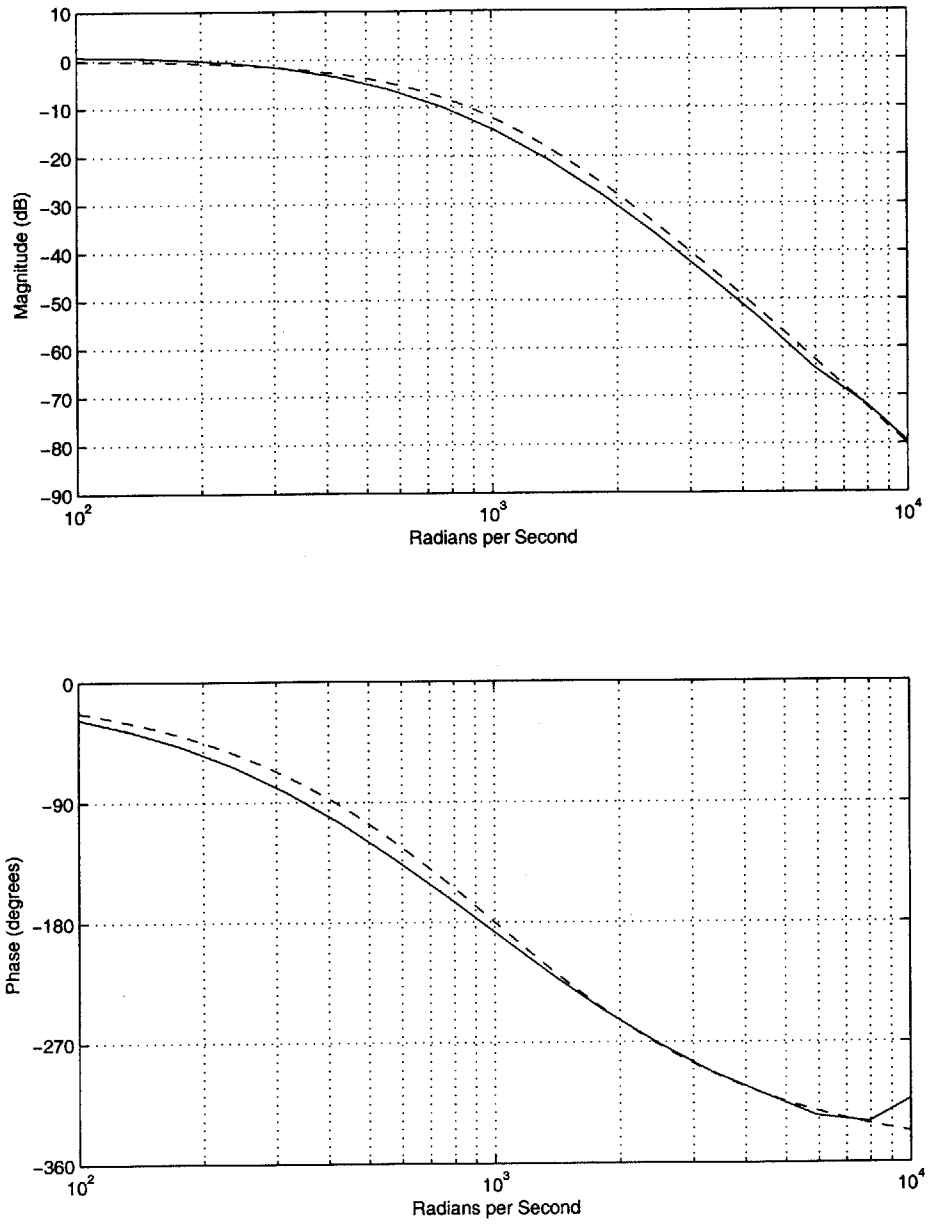

Figure 2-6: Measured versus expected results.

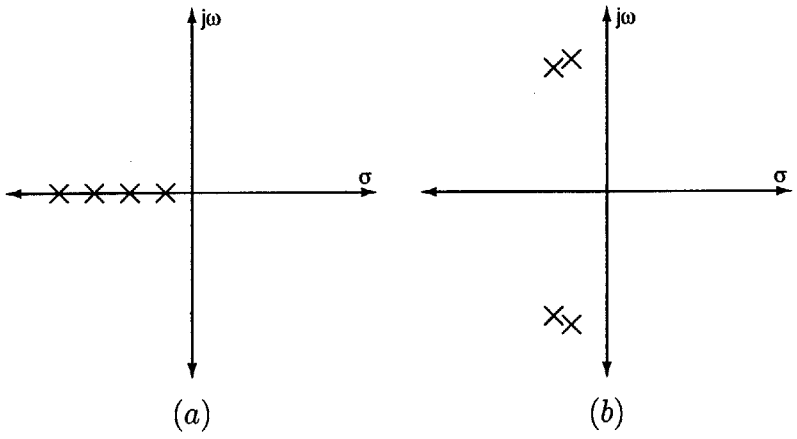

Figure 2-7: Example assignment systems.

2.6 Future Work

While the current hardware works well, there are some areas where future efforts should be directed. In specific, the experiment phase measurements are not perfectly ideal, and the system is limited by the dynamic range of the multiplier ICs.

The state-variable filter uses feedback loops to implement the various canonical second-order responses desired. The ideal results of these feedback loops do perfectly match the responses of the desired systems, but in practice the measurements are not ideal. This error stems from the operational amplifier's high-frequency, parasitic pole. This pole negatively affects the high-frequency performance of each integration, and compounds due to the four amplifiers present in the forward signal path. This non-ideality is most obvious upon careful inspection of the phase data. The multiple parasitic poles present additional negative phase several decades below the actual parasitic location.

Phase error can possibly improve with higher-performance operational amplifiers, but this solution is both costly and trivial — it is always the case that higher-performance parts can provide some relief. Another, more practical solution is the addition of lead compensators in series with the integrators. The lead compensation provides a positive phase "bump" at the geometric mean of the compensator. If the bump is placed near the location of the parasitic op-amp pole, then the measured

phase error should be improved.

Dynamic range should also be further investigated. The current system can only provide a linear range of ω_n and ζ between 0 and 5 V. The resolution of the LabJack^{TM} and the digital-to-analog converters means that practically the dynamic range of possible values is no better than two decades. A logarithmic relationship between command voltage and circuit parameters would enable a greater range of responses possible, but likely expose the limits of saturation and frequency performance throughout the rest of the state-variable filter. In other words, proceed with caution.

2.7 Conclusion

Web-based laboratories are useful educational tools because they essentially provide a "control" with which to compare the knowledge of every student. Weblabs also streamline the students' learning process by allowing them to skip the tedious circuit tasks invovled with building a specific system, while still utilizing the actual, measured results from a real-world system.

Weblabs, however, are limited by the hardware which executes the experiment. While building customizable, settable systems is often possible, the dynamic range and practical performance of such circuits can sometimes cause problems.

For the purposes of this experiment, however, the state-variable filter does prove to be robust, smooth and an all-around worthy solution. While possibilities do exist which can expand its functional range and improve its system model, the current system will go into immediate use and hopefully save future students the continued trauma of boring start-of-term review.

Chapter 3

Magnetic Levitation System

3.1 Introduction

Magnetic levitation is an often-used demonstration for feedback systems courses due to its challenging open-loop instabilities and impressive closed-loop behavior. Levitation systems are both difficult to build and expensive to assemble. The systems require a coil to generate an upward magnetic field, an object for levitation, and a position sensor.

In many class demonstrations the position sense is achieved with a light bulb and photodiode. The closed-loop system controls the position of the levitated object to some fixed intensity of light at the photodiode — as the object moves closer to the coil, light intensity decreases, while if the object moves away from the coil, the light intensity increases. This position sensor provides the necessary information to provide the overall system with negative feedback.

This setup, however, is too expensive and elaborate for many students to build on their own for a class project. To meet the requirements of cheaper cost and less overall complexity, a unique and different kit must be assembled.

A new magnetic levitation kit for students has been recently developed that uses a Hall-Effect sensor and H-bridge circuitry to bring the cost down to less than $20 [12, 13]. The Hall-Effect sensor detects the present magnetic field, and can therefore provide some sense on the position of a levitated object with a permanent magnet

attached.

This system is not without its own drawbacks, however. The sensor is corrupted by the magnetic field generated by the coil, making stable behavior a very initial-condition dependent endeavor. Furthermore, the H-bridge circuitry, while simple for students to configure, is a large portion of the $20-kit cost. Students often attain stability with a varible-gain in the sensor's feedback loop, as well as painstaking trial-and-error routines concerning the size and weight of levitated objects.

This chapter will explore the possibilities of improving this current system with better position sense and cheaper power electronics. Slight modifications and approaches will result in a final kit cost closer to $10, and another interesting result.

3.2 Analysis

Magnetic levitation derivations are not difficult to find, and they reveal a very expected result [14]. The levitation system consists of a right-half-plane zero and a left-half-plane-zero distributed evenly on either side of the origin. The pole locations are dependent on the mass of the levitated object, the necessary DC coil current necessary for equilibrium, and the distance below the coil the object will levitate. This result is not particularly useful in the construction of cheap magnetic levitation kits because some parameters are difficult to determine, and for the cost spent it is difficult to find parts with reliable characteristics. Furthermore, most demo systems are not concerned with transient behavior or dynamic range; they are simply designed to work for one standard setup [14].

One practical solution to this analysis issue, and something that has already been implemented by many students and encouraged by course staff, is to build the basic system and use measurements of the closed-loop system to determine what compensation is necessary to stabilize the system. Basic root locus reveals that in a feedback loop the two poles will meet at the origin and travel along the $j\omega$-axis. This closed-loop system is not stable, but should be marginally stable enough to allow students to measure the damping frequency of the closed-loop response.

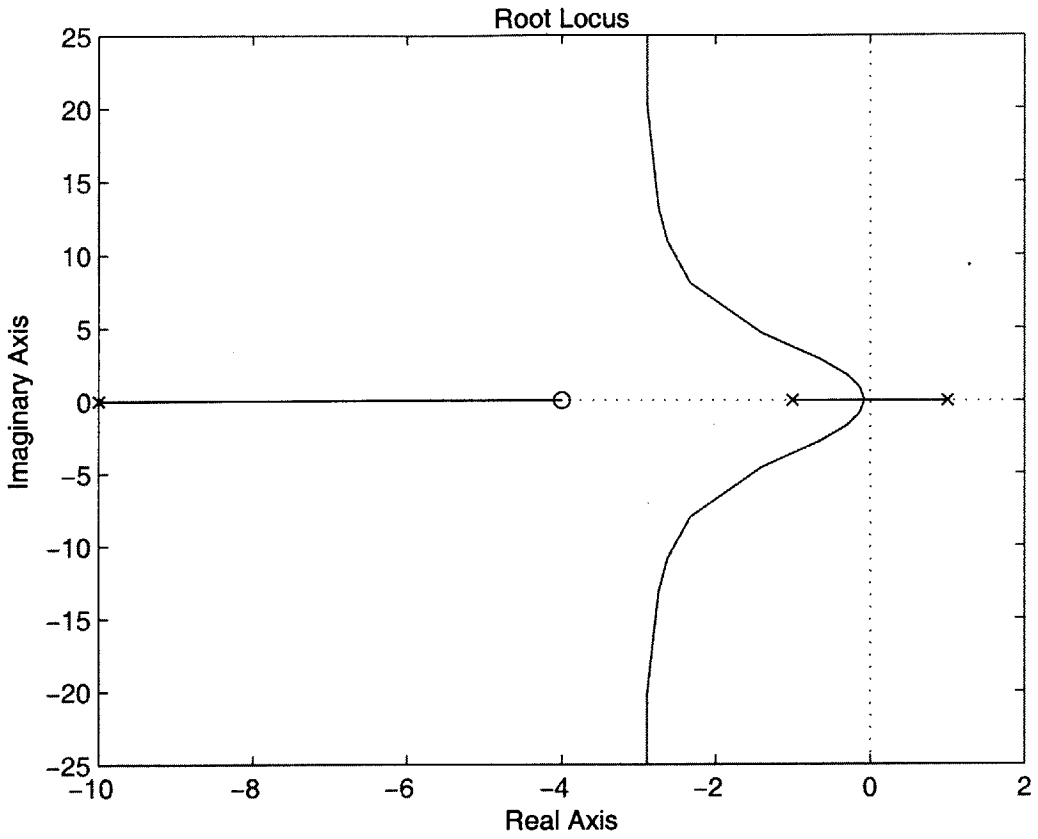

Figure 3-1: Example root-locus of magnetic levitation system with series lead compensation. Lead compensation uses conservation of centroid to stabilize conjugate pair.

With this information students are able to design a lead compensator to improve the stability of the system. The lead compensator moves the centroid into the left-half plane and thus pulls the two system poles into a stable region. An example of this root locus is illustrated in Figure 3-1.

3.3 Design

The $10 levitation kit was compensated in a similar manner as the previous versions, with a variable gain amplifier in series with the Hall-Effect sensor and a lead compensator, which drives the Micrel fan chip. The kits differ from the previous version, however, because the fan chip now merely drives a simple transistor configured to drive current through the electromagnetic coil, thus eliminating the costly H-bridge

circuits. This power drive approach was first suggested by [15, 16]. Figure 3-2 illustrates the modified controller circuitry which incorporates the new power electronic scheme.

This plug-and-play solution is viable because the Micrel fan chip is actually optimized to drive transistors.

3.4 Results

A levitation system was built and tested as described, with a final kit cost of $10. Additionally, with proper attention to the loop gain of the system, the kit is capable of suspending objects *without* a permanent magnet attached. This capability is a subtle side-effect of the Hall-Effect sensor. The proximity of a metal object beneath the coil actually effects the number of magnetic field lines passing through the sensor, and therefore the sensor provides a small amount of feedback even without a magnet present. A controller system with high enough loop gain can therefore levitate metal objects without needing permanent magnets.

3.5 Future Work

While the Hall-Effect sensor remains one of the keys to a cheap levitation system, its difficult and nonlinear behavior remains a big obstacle for the realization of better stability and general levitating behavior. Future work in cheap levitation should include a thorough investigation of the true behavior of this sensor. A totally automated system could be achieved if an understanding of the nature of the position sense existed. Future work could include a proper modeling and linearization of the Hall-Effect sensor.

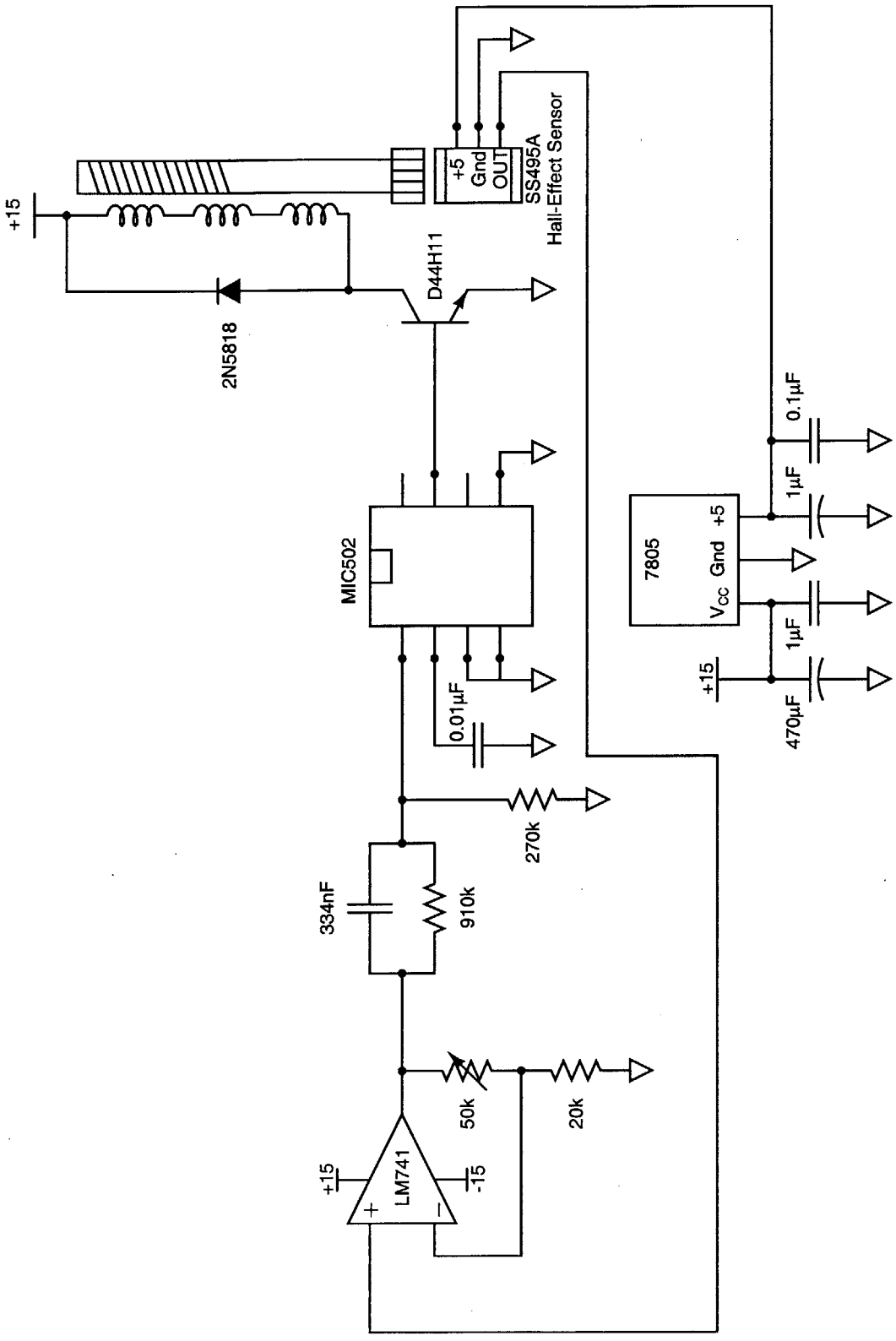

Figure 3-2: Magnetic levitation controller and drive circuitry. D44H11 replaces previous H-bridge circuitry and matches previous performance while reducing cost severely.

3.6 Conclusions

Cheap magnetic levitation can be achieved similar to previous kits with the addition of a single transistor coil drive. Further, the need for permanent magnets can be negated with careful attention paid to feedback-loop gain.

Chapter 4

Inverted Pendulum System

4.1 Introduction

The stabilization of the inverted-pendulum system, illustrated in Figure 4-1, is an often-used demonstration in many control and feedback systems courses. At MIT, the inverted-pendulum demonstration is a traditional favorite amongst students, while recently developing into a headache for department staff that worsens in intensity and duration with each passing semester. The inverted-pendulum now exists as a phantom, making appearances in lecture and working tenuously while reserved lecturers force a smile, or appearing in lecture but being quickly abandoned to the corner of the hall while teased students take notes and wonder when or if the demo is going to be shown.

The demonstration can be made to work for a few moments, but no longer continuously. The demonstration can be having a "good day," but the sensors for pendulum angle or cart postion may fail at any moment and without warning or provocation.

The fact that the schematic is not shown to students is not to maintain some department or trade secret, but rather as a safety measure to preserve what students have already learned. The truth is nobody really knows why or how the systems works while it is behaving, and certainly nobody knows the reason when it fails. For a long time the system just plain worked, and this bottom line combined with its recent deterioration has quickly made it the prodigal son of the MIT Electrical Engineering

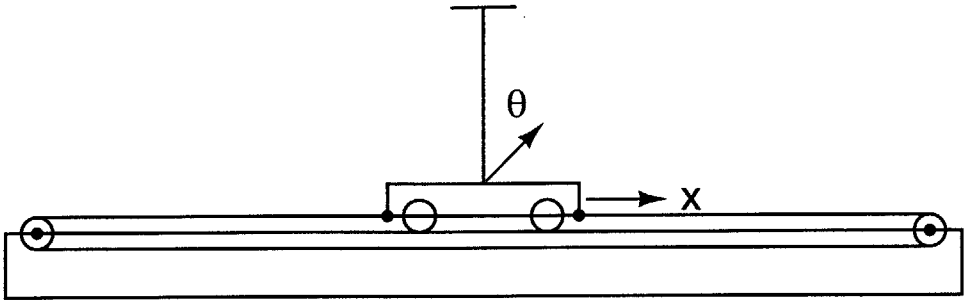

Figure 4-1: Inverted-pendulum system. Motor drives right-hand-side pulley and position sense mounts on the left-hand-side pulley. Track length and pendulum length are 1.75 meters and 0.40 meters, respectively.

and Computer Science department.

This chapter will review the analysis of the system, implement new sensors for angle and position, and attempt to rebuild the control with a well-known solution that can restore the department's inverted-pendulum system to its past glory and once robust behavior.

4.2 Analysis

4.2.1 Inverted Pendulum System

The inverted pendulum demonstration is similar to what is pictured in Figure 4-1. The total track length is 1.75 meters, and the cart is driven by a motor which drives the right-hand-side pulley. Braided cord connects to either end of the cart and around the driven pulley and the free-spinning pulley. A position sensor is placed on the axle of the free-spinning pulley, and an angle sense is placed at the hinge of the inverted pendulum.

Using the parameter and sign definitions from Figure 4-1, the angular acceleration of the pendulum is equal to $(g/l)\sin\theta$, while a cart acceleration of $\ddot{x}$ generates an angular acceleration of $-(\ddot{x}/l)\cos\theta$. These relations can be combined and linearized to generate a simple, linear model of the system for small perturbations in θ.

The angular equation of motion for the inverted pendulum is

$$\ddot{\theta} = (g/l)\sin\theta - (\ddot{x}/l)\cos\theta. \tag{4.1}$$

The presence of the trigonometric functions sine and cosine in Equation 4.1 mean that this differential equation is not linear. Assuming, however, that the pendulum angle will always be nearly zero, the small-angle approximations can be substituted to yield a linear differential equation. For small θ, $\sin\theta \approx \theta$ and $\cos\theta \approx 1$, yielding the linear equation

$$\ddot{\theta} = (g/l)\theta - (\ddot{x}/l). \tag{4.2}$$

Taking the Laplace Transform of this linear differential equation generates the system transfer function $G(s)$, describing the small-signal response of pendulum angle for small-signal changes in cart position

$$\begin{aligned} s^2\Theta(s) &= (g/l)\Theta(s) - s^2X(s)/l & (4.3)\\ \Theta(s)(ls^2 - g) &= -s^2X(s) & (4.4)\\ \frac{\Theta(s)}{X(s)} &= \frac{1}{g}\left(\frac{-s^2}{\tau_L^2 s^2 - 1}\right) & (4.5)\\ G(s) &= \frac{\Theta(s)}{X(s)}, & (4.6) \end{aligned}$$

where $\tau_L = \sqrt{l/g}$. The length of the pendulum is approximately 40 cm, making $\tau_L = 0.2$ s.

4.2.2 Motor Drive

The cart will be driven by a DC motor via two pulleys and a braided cord. The braided cord is secured to both sides of the cart and is wrapped around both the free-wheel pulley and the motor-driven pulley. The specific motor transfer function, relating input voltage to output shaft angle, is

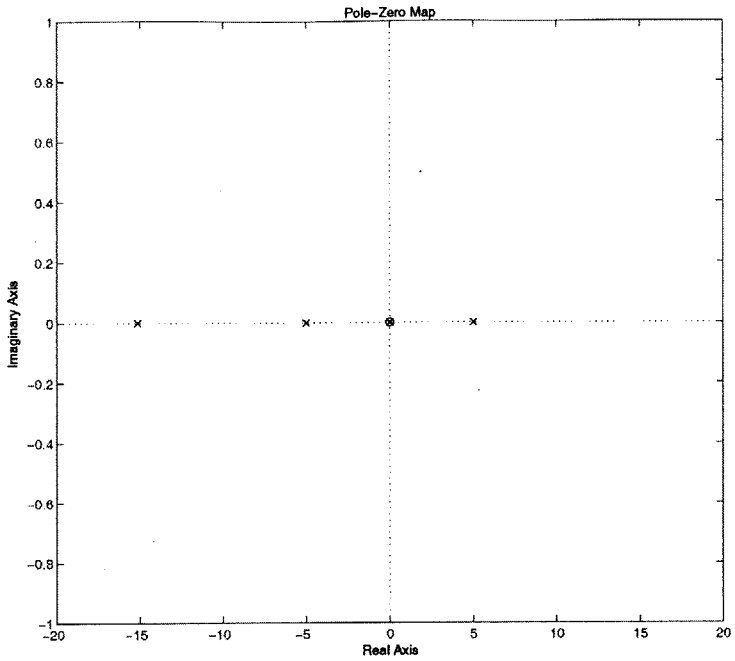

Figure 4-2: Pole-zero plot of $G(s)M(s)$. Two zeroes at the origin create difficult locus trajectories for right-half-plane poles.

$$M(s) = \frac{\theta_{\text{motor}}}{V(s)} = \frac{4.87}{s(0.066s+1)} \left[\frac{\text{rad}}{\text{V}}\right]. \tag{4.7}$$

The angle-to-position coefficient, $1/n$, as well as the tachometer coefficient, k_{TACH}, are measured as

$$\frac{1}{n} = 0.0318 \left[\frac{\text{m}}{\text{rad}}\right] \tag{4.8}$$

and

$$k_{\text{TACH}} = 0.16 \left[\frac{\text{V}}{\text{rad/s}}\right]. \tag{4.9}$$

These functions lead to an open-loop system characterized by the pole-zero plot in Figure 4-2. The right-half-plane pole as well as the two zeroes at the origin make this compensation a particularly unique challenge. This system is both open-loop and closed-loop unstable.

4.2.3 Angle Sense

The new angle measurement for the inverted pendulum will be produced by a continuous-turn servo-potentiometer mounted at the inverted pendulum's hinge. The potentiometer is set such that a vertical pendulum produces 0 volts, while positive angles produce a negative voltage proportional to the supply voltage. Since the pendulum can swing a maximum of π radians, this angle sense can utilize half of the power supply range. The old system setup used a 10-turn potentiometer at the same location, meaning that it only used one-twentieth of the full range.

With a supply voltage of 15 volts, the angle coefficient is

$$K_\theta = -4.77 \left[\frac{\text{V}}{\text{rad}}\right]. \tag{4.10}$$

Note the negative sign of K_θ; this polarity is due to definition of the system and implementation of the sensor. Most likely, the original system called for $-\theta$, and this reversal is an easy way to avoid an additional inverting amplifier in the controller.

4.2.4 Position Sense

A 10-turn trim potentiometer was also used in the old system's position sense. In general, trim potentiometers are not meant for servo applications, and therefore the potentiometer can fail during continuous use due to internal contact failures.

Since the potentiometer is mounted to the free-spinning pulley opposite the motor — and is, therefore, coupled to position via the angle-to-position coefficient of Equation 4.8 — a similar continuous-turn servo-potentiometer cannot be used to sense position since several rotations are required as the cart moves from one end of the track to the other.

One solution is to use an extra gear which down-samples the free-wheel pulley rotations and places the servo-potentiometer on the extra gear. This solution, however, is costly and requires the kind of mechanical expertise and time that Course VI staff are unable to provide and maintain.

An electrical solution is to use an optical encoder, which is a digital sensor that

produces pulses proportional to pulley rotations. An encoder can be chosen with the correct pulse rating to simulate the effect of down-sampling.

While the design of the encoder circuitry will be explained later, enough information already exists to determine the position sensor coefficient. The encoder chosen produces 256 pulses per one revolution of the free-wheel pulley. A 12-bit binary counter counts these pulses and a digital-to-analog converter produces a ±10-volt output. The total output swing of the DAC is therefore

$$\frac{1}{0.0318}\left[\frac{\text{rad}}{\text{m}}\right] \times \frac{256}{2\pi}\left[\frac{\text{bits}}{\text{rad}}\right] \times \frac{\pm 10}{2^{12}}\left[\frac{\text{V}}{\text{bits}}\right] \times 1.75\,[\text{ m}] = \pm 5.5\text{ V}, \tag{4.11}$$

where the total length of the track is 1.75 meters. Since the output swings only ±5.5 volts from the center of the track to the endpoints, the output is doubled with a separate LF411 amplifier, leading to a final position coefficient of

$$K_X = 12.6\left[\frac{\text{V}}{\text{m}}\right]. \tag{4.12}$$

Since the track spans 0.875 meters from the center to the endpoints, this means that the position sensor will generate an analog voltage that swings ±11 volts from center to end.

4.2.5 Final System Model

With the pendulum system, motor drive and sensors completely analyzed, Figure 4-3 illustrates the entire open-loop system. Coefficients with an "M" subscript indicate a parameter measurement, and are thus a voltage.

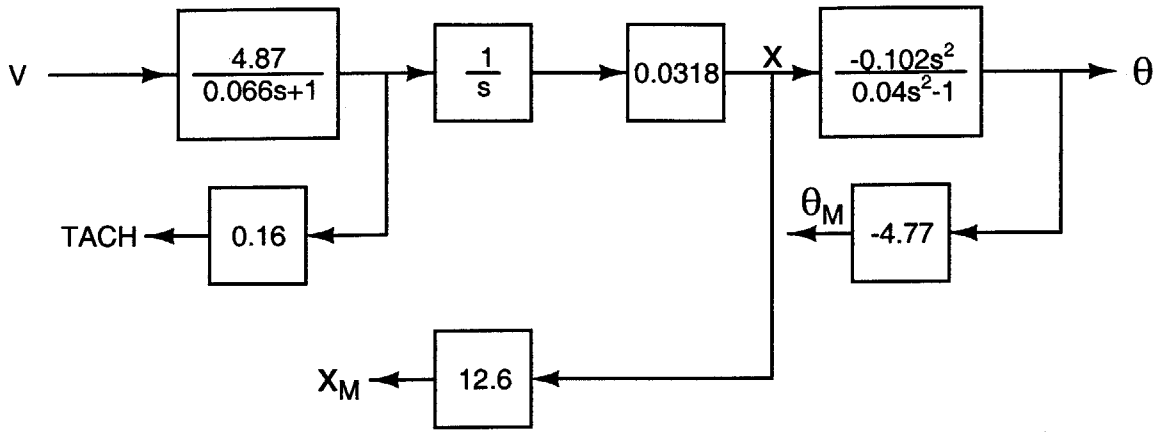

Figure 4-3: Complete inverted pendulum open-loop system. "M" subscript denotes a voltage measurement of the system parameter. Natural integration occurs between motor shaft speed and motor shaft angle.

4.3 Design

4.3.1 Optical Encoder Design

Since feedback systems courses are mostly taught using analog systems and analog electronics, the most important aspect of the optical encoder design — a digital system — is that it functions reliably and without attracting attention to itself. The encoder should simply provide a voltage proportional to the position of the cart on the track, and nothing more.

Of course, since this sensor is digital its output will not be continuous, but rather a staircase of voltage where step-size relates to the resolution of the system. As mentioned before, the encoder divides the track into 2242 equally-sized pieces (1281 bits per meter). The track length is 175 cm, so the resolution of a 256-pulse encoder is 781 μm. This step-size should be sufficient for the controller.

As shown in Figure 4-4, the topology of the sensor includes the encoder, a quadrature detector, a 12-bit counter, and a digital-to-analog converter. The optical encoder outputs two signals in quadrature; meaning that one signal leads the other by 90°

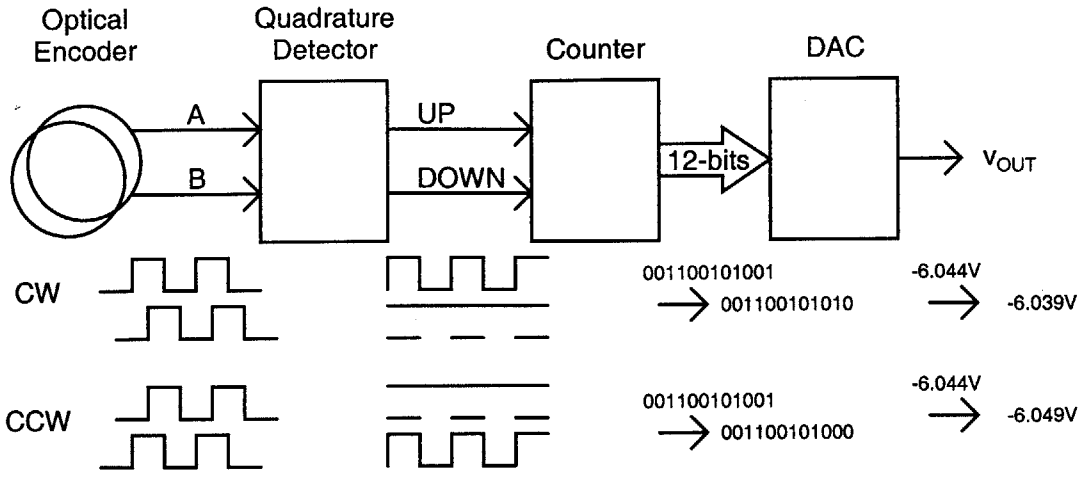

Figure 4-4: Optical encoder sense diagram. Encoder controls two signals in quadrature, which are decoded into `UP/DOWN` pulses and counted with 12 bits before analog conversion.

during clockwise revolutions, while the opposite is true for counter-clockwise revolutions. The quadrature detector senses the direction of movement, and controls two signals, sending pulses on the `UP` line while the encoder rotates clockwise (in the positive x direction), or sending pulses on the `DOWN` line while the encoder rotates counter-clockwise (and in the negative x direction). A 12-bit up/down counter is a standard part found in most digital logic families which counts from 0 to 4095. The counter should be initialized to 2047 so that it counts equally up and down from the center point of the track. This initialization means the cart must be centered during power-up to properly configure the counters. The digital-to-analog converter converts the counter output into an analog voltage, which is sent to the controller as the analog measurement.

This circuitry is implemented using the standard `SN74LS` family of digital products (Figure 4-5). The AD767 by Analog Devices serves as the 12-bit digital-to-analog converter, and is configured to offset the output so the middle of the track corresponds to ground, while the ends of the track correspond to ± 11 V.

The circuitry sufficiently substitutes for the old 10-turn potentiometer, and should survive the test of time; allowing instructors to now run the demonstration continuously and without fear that the contacts within the potentiometer will corrode and

fail at any time.

4.3.2 Pendulum Controller

Overview

The compensation approach demonstrated here reflects the theoretical solution annually taught in 6.302 Feedback Systems. This compensation methodically tackles the various difficulties inherent in stabilizing an inverted pendulum system.

The basic stability problem stems from the inverted pendulum system function derived in Equation 4.5 and repeated here in Equation 4.13:

$$\frac{\Theta(s)}{X(s)} = \frac{1}{g}\left(\frac{-s^2}{\tau_L^2 s^2 - 1}\right) = \frac{-0.102s^2}{0.04s^2 - 1}. \tag{4.13}$$

This system introduces two zeroes at the origin and two poles distributed around the origin at $s = \pm 5$ rad/s. The zeroes are particularly difficult during compensation because in feedback closed-loop poles approach the open-loop zero locations. Therefore, the only way to "pull" the right-half-plane zero into the left-half-plane is to introduce a second unstable pole — otherwise the unstable pendulum pole would simply approach the origin from the right under feedback, and the system would never be stable.

Positive feedback around the motor moves its integration pole off the origin and into the right-half-plane; essentially, positive feedback means that the only equilibrium point is a vertical pendulum at the center of the track. Otherwise, the system would stabilize the angle but run right off the end of the track. Further, the addition of a lag compensator with a low-frequency pole and a zero at $s > 5$ rad/s results in the root-locus plot of Figure 4-6. This controller strategy is the exact compensation scheme proposed in feedback courses and is thus a "textbook" solution to the inverted pendulum problem. If an actual controller used this scheme, it would enhance the value of the approach's educational value.

The general block diagram which implements this feedback topology is illustrated in Figure 4-7. The controller design is performed from the inner-most loop to the

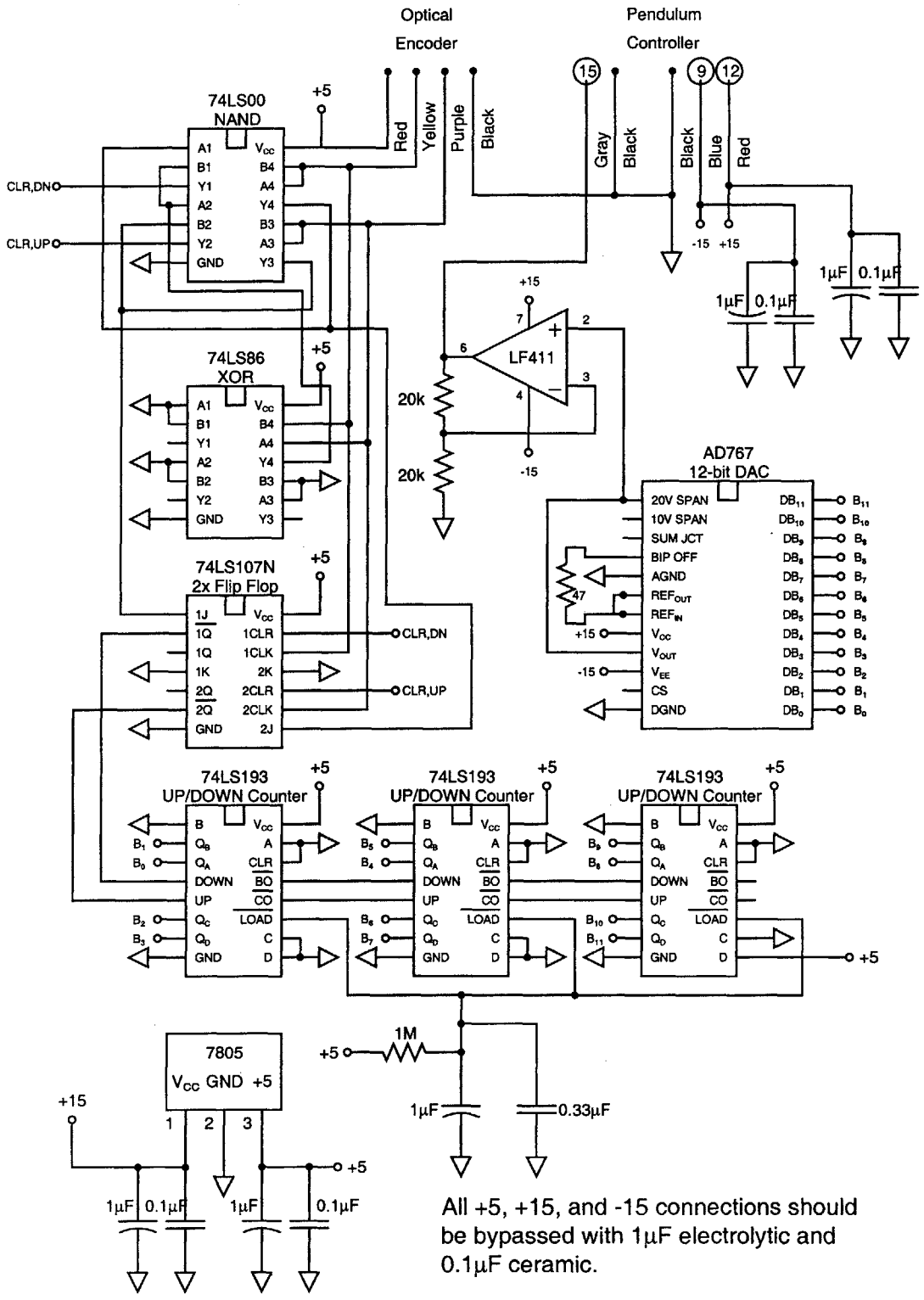

Figure 4-5: Decoder schematic. Pendulum controller makes five connections and the optical encoder makes 4 connections. Four-bit counters cascade to implement 12-bits, and the LF411 doubles the output range of the AD767.

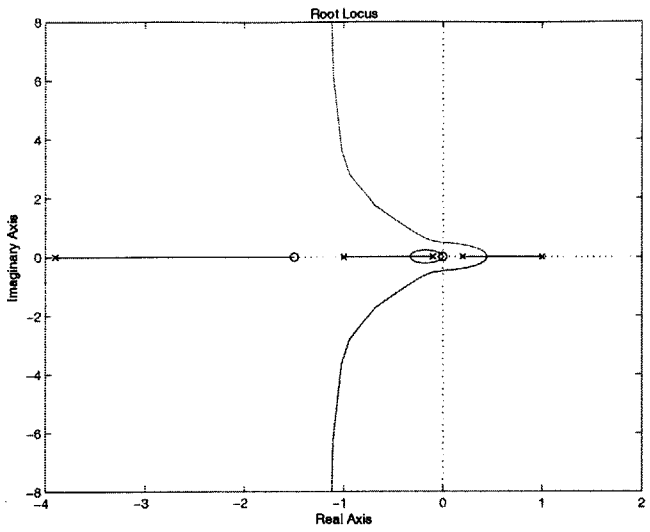

Figure 4-6: Root-locus plot demonstrating inverted pendulum compensation. This plot appears verbatim in 6.302 inverted pendulum lecture slides.

outer-most loop. The inner-most loop is velocity feedback around the motor, and the closed-form of this loop is described by

$$\frac{\dot{\Theta}_{\text{MOTOR}}}{V_2}(s). \tag{4.14}$$

Velocity feedback serves to provide motor speedup, enhancing the motor's ability to follow input-voltage transients. It is not absolutely required to ensure system stability, but as the motor pole gets faster, the system becomes more stable via the centroid conservation root-locus rule. The next loop is positive feedback around the motor. This loop must include the angle of the motor shaft, and is therefore taken around the cart position — since position is proportional to motor shaft angle via the pulley/wire coupling. The closed-form of this loop is described by

$$\frac{X}{V_1}(s). \tag{4.15}$$

This positive feedback loop forces the motor's integration pole into the right-half plane. The final feedback loop is the actual negative feedback around the pendulum angle

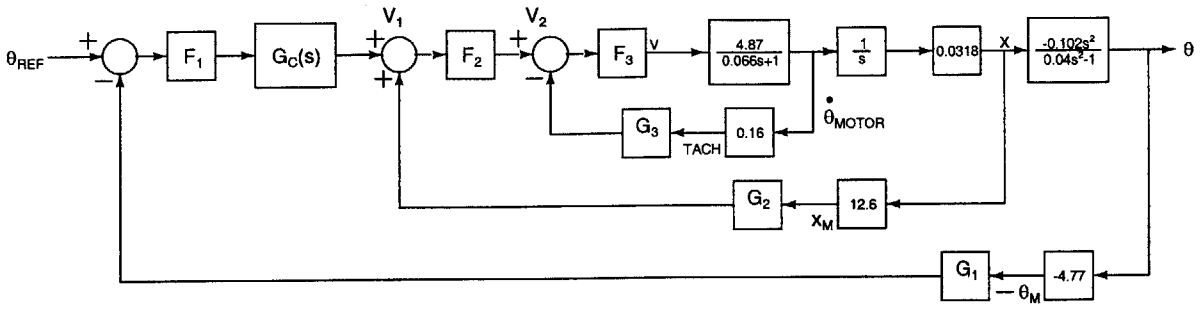

Figure 4-7: Basic compensation topology. Topology distributes loop gain between the forward path F_n and the feedback path G_n.

$$\frac{\Theta}{\Theta_{\text{REF}}}(s). \tag{4.16}$$

The system will be driven by the error voltage created by the first summing block in the feedback topology.

What follows is a step-by-step design of these three feedback loops.

6.302 Inverted Pendulum Controller Design

While there is no theoretical limit to how fast the velocity-feedback loop can make the motor's speed response (see Figure 4-8, the velocity-loop root-locus), there are physical limits in the motor and gain limitations in the other feedback loops. The farther out the motor pole is set by the velocity-feedback loop, the more gain required in the outer-most loop to pull the right-half-plane poles into the left-half plane.

By solving for the closed form of the velocity loop, the new pole's time constant and DC gain can be written explicitly:

$$\text{DC Gain} \;=\; \frac{4.87 \times F_3}{1 + F_3 G_3 \times 0.16 \times 4.87} \tag{4.17}$$

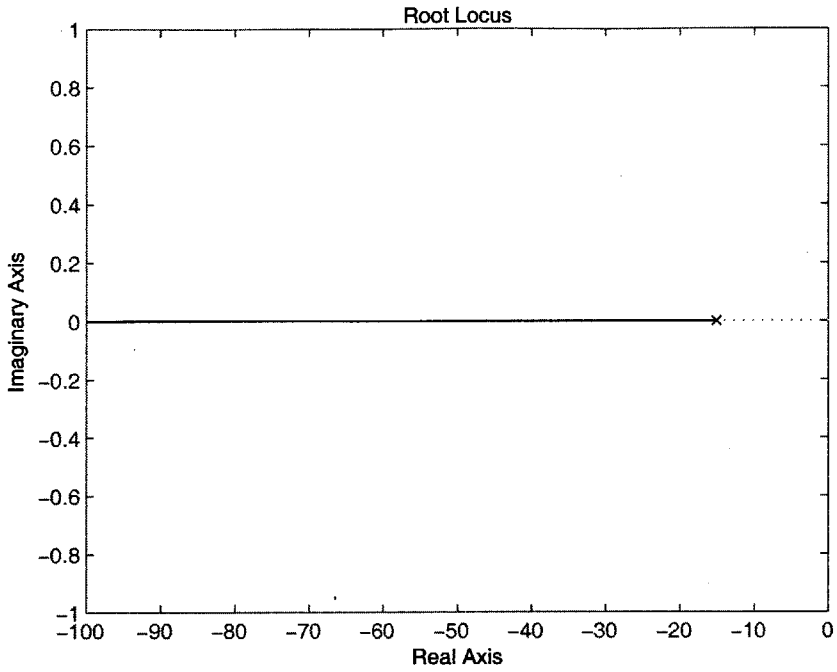

Figure 4-8: Root locus plot of velocity feedback loop. Unlimited speed is possible in theory, not in practice.

$$\tau = \frac{0.066}{1 + F_3 G_3 \times 0.16 \times 4.87}. \tag{4.18}$$

Equation 4.17 demonstrates that by splitting the total loop gain between a forward and feedback gain, the DC gain can be set independently of the motor pole. Tracking the DC gain of the closed-form is critical to the design of outer feedback loops.

Ultimately the loop gain F_3G_3 was set by observing the tachometer response on an oscilloscope. Once the speed response appeared to slew, the motor was at its limit and further increases in loop gain would be wasteful. This pole location did not seem too fast for later feedback loops, and the split loop gain topology served to distribute the later feedback-loop-gains more evenly. Figure 4-15 reveals that $F_3 = 1.5$ and $G_3 = 8$. This leads to the closed-loop solution described by

$$\frac{\dot{\Theta}_{\text{MOTOR}}}{V_2}(s) = \frac{0.706}{0.0064s + 1} \left[\frac{\text{rad/s}}{\text{V}}\right]. \tag{4.19}$$

The next loop to design is the positive feedback around controller voltage $V_1(s)$ and cart position $X(s)$. Cart position is sensed through the optical encoder and

the measured result is a voltage signal x_M. A complete understanding of the sensor behavior is critical during controller design, as the sensor coefficent of 12.6 [V/m] appears in the feedback loop.

The cart-position loop includes the inner loop solved in Equation 4.19 and the natural integration inherent in the translation from motor-shaft speed to motor-shaft angle. It is this pole that the positive feedback needs to push into the right-half plane. Experimentation with the total root-locus plot in Figure 4-6 reveals that this low-frequency right-half plane pole must be closer to the right-hand pendulum pole than the low-frequency left-half plane pole is to the left-hand pendulum pole. If the left-side poles are closer to each other than the right-side poles, then the left-half plane poles will asymptote at the centroid, leaving the right-hand poles to asymptote into the origin, having never reached the left-half plane.

The loop gain F_2G_2 must therefore be large enough to move the integration pole beyond the value of the left-half plane pole, which is introduced by the series compensator $G_C(s)$ in the angle loop. The limitation here is that the compensator pole will be developed through some filter, and is limited by the quality and size of capacitors available. The highest performance capacitor available is 0.33μF, and thus the compensator pole location is $s = -0.827$ rad/s. The natural integration pole must therefore exceed $s = 0.827$ rad/s in the closed-loop.

The quadratic formula is employed to explicitly solve the closed-loop pole locations of the cart-position feedback loop

$$s_{1,2} = \frac{-1}{2\tau_1} \pm \frac{\sqrt{1 + 4\tau_1 a_1 F_2 G_2 \times 12.6 \times 0.0318}}{2\tau_1}, \tag{4.20}$$

where $\tau_1 = 6.38$ ms and $a_1 = 0.706$ from Equation 4.19. Note that if $F_2G_2 = 0$, then the pole locations are simply $s = -157$ and $s = 0$, exactly the open-loop behavior — this provides a check to ensure the math is correct. The root-locus plot (Figure 4-9) of the cart-position loop also affirms the behavior described in Equation 4.20; namely that high loop gain results in pushing the integration pole further into the right-half plane.

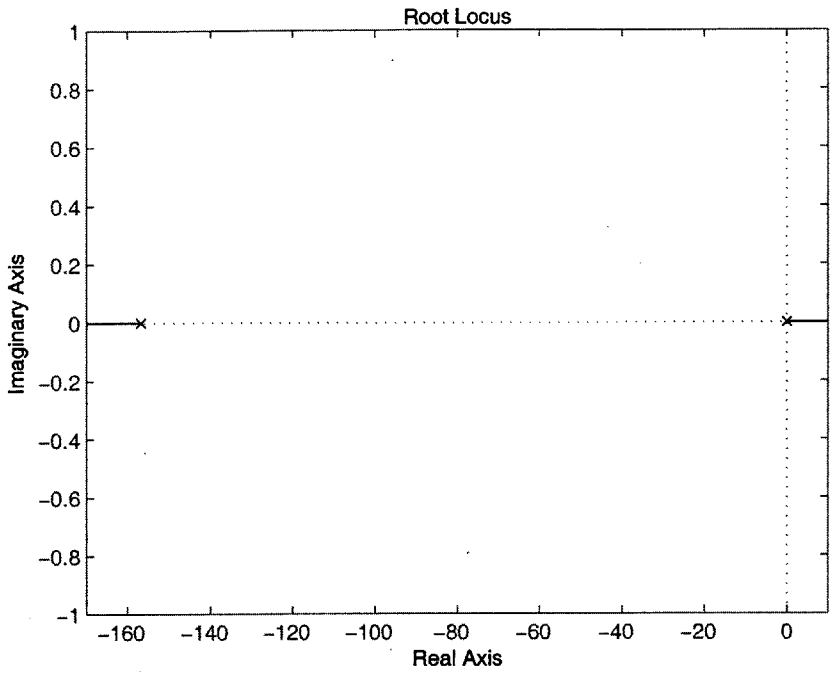

Figure 4-9: Root-locus plot of cart-position feedback loop. Positive feedback forces the motor's $s = 0$ pole into the right-half plane.

This design set F_2G_2 such that the right-hand pole exceeded $s = 0.827$ rad/s with plenty of margin. The schematic distributes the loop gain between F_2 and G_2 such that voltage levels remain adequately within the supply voltages. $F_2 = 21.4$, $G_2 = 0.373$ and the resulting pole locations are

$$s_1 = -159 \text{ rad/s} \tag{4.21}$$

and

$$s_2 = 2.23 \text{ rad/s}. \tag{4.22}$$

Note that G_2 is set by the resistor divider at the input of the noninverting op-amp in Figure 4-15. F_2 is set by the gain of the noninverting op-amp and the following inverting op-amp configuration:

$$G_2 = \frac{100\text{k}}{89\text{k}} \times \frac{100\text{k}}{100\text{k} + 200\text{k}} = 0.373 \tag{4.23}$$

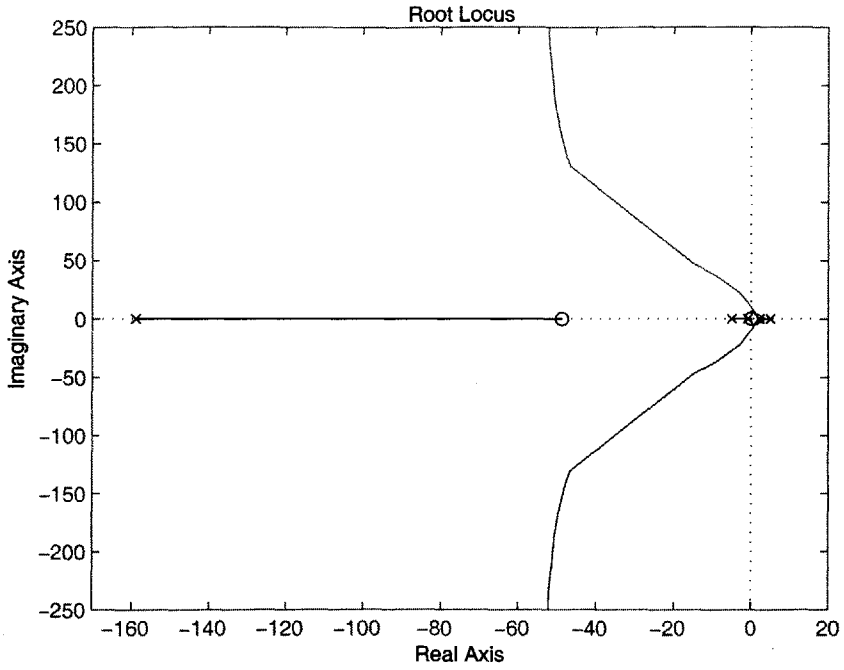

Figure 4-10: Final pendulum system root-locus plot. Real system closely matches the lecture slide in Figure 4-6.

and

$$F_2 = \frac{1.1\text{k} + 15\text{k}}{1.1\text{k}} \times \frac{120\text{k}}{82\text{k}} = 21.4. \tag{4.24}$$

The final design steps necessary are to design a series lag compensator and to set the final loop gain F_1G_1. The compensator pole is basically maximized with a time constant set by a 3.6MΩ resistor and the aforementioned 0.33μF capacitor. At first glance the only constraint on the zero location is that it must be between the motor's pole and the pendulum's left-hand pole. Root-locus examinations, however, reveal that the proximity of the zero to the motor pole has some determining factor behind which conjugate pair of poles asymptote to the centroid. A zero location was determined to ensure that the proper conjugates asymptote. The final loop root-locus plot confirms that this design has sufficiently guaranteed stability while following the 6.302 "textbook" design scheme. Figure 4-11 expands the region near the origin to check that the right-hand poles do in fact stabilize.

Once it is confirmed that this loop provides a stable solution, a Nyquist plot

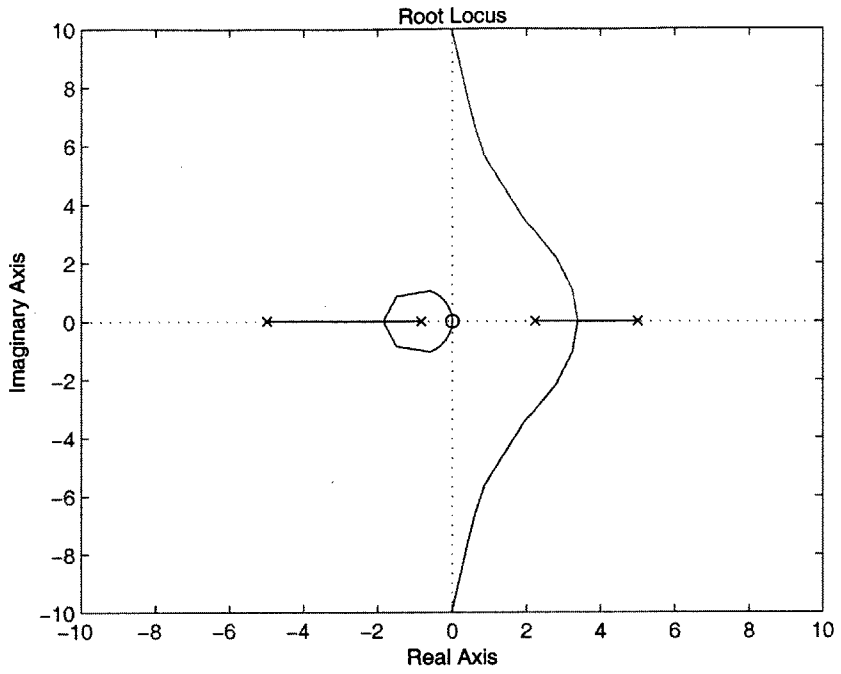

Figure 4-11: Enlarged root-locus plot for final system, illustrating that in fact the unstable poles asymptote in a stable region.

can confirm if the system is stable with the loop gain established. G_1 was set to guarantee that the system would constrict the pendulum angle to $\pm 5°$. F_1 consists of the compensator's DC gain and the resistor divider at the input of the noninverting amplifier. The resulting loop gain is

$$F_1 G_1 = 68.9. \tag{4.25}$$

The Nyquist plot for this final system confirms that this system contains two negative encirclements of the -1 point, thus offsetting the two right-half-plane poles in the open-loop system and establishing that the closed-loop system has no right-half-plane poles. Figure 4-12 is the complete Nyquist plot and Figure 4-13 is an enlarged view of the -1 point. The Bode plot in Figure 4-14 concludes that the system has a phase margin near 25°, which is close to the maximum for this compensation approach.

Figure 4-15 is the controller circuit which implements the design described here.

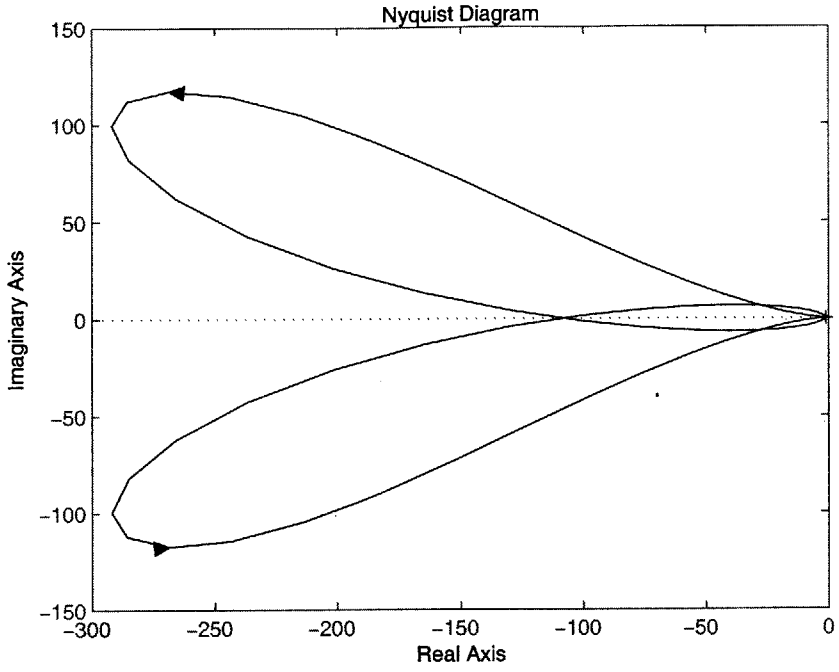

Figure 4-12: Nyquist plot. Nyquist confirms that there are three regions of operation, with 0 encirclements, -2 encirclements and 0 encirclements, as confirmed on the root-locus plot of Figure 4-11. Negative encirclements cancel the 2 positive encirclements of the D-contour in the open-loop system, thus ensuring stability in this region.

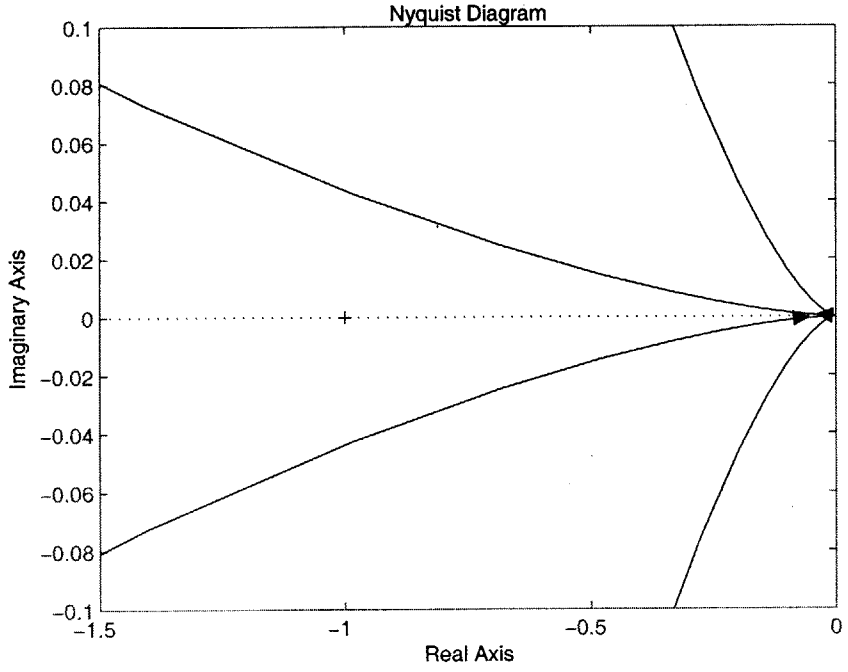

Figure 4-13: Enlarged nyquist plot. There are 2 negative encirclements of the -1 point.

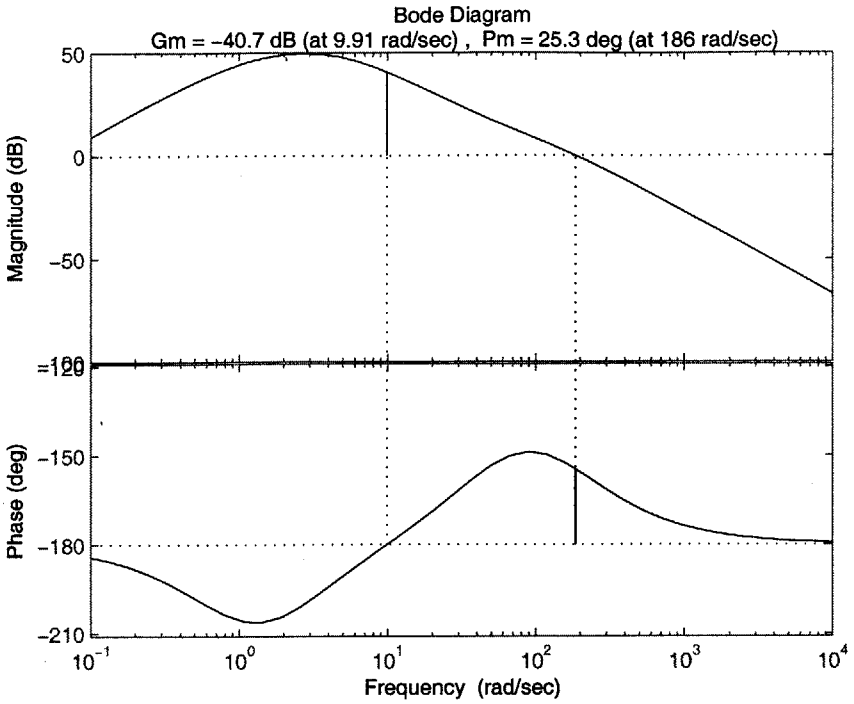

Figure 4-14: Bode plot for final pendulum system. A crossover of 186 rad/s is close to the maximum phase margin possible.

4.3.3 Former Pendulum Controller Modifications

Despite the changes to the sensors, the previous controller should still be operational if efforts are made to ensure that sensor behavior remains consistent.

The position sensor does exactly match the old 10-turn potentiometer solution. The 10-turn potentiometer produced ± 10 volts at the endpoints of the track, which is similar enough with the new optical encoder sensor to not require any modification.

The angle sensor, however, does require some modification. The new potentiometer produces 10 times the voltage for the same pendulum angle. The old controller was modified to reduce the gain in series with only the angle sense by a factor of 10, thus maintaining the same overall behavior.

Another observation of the old pendulum controller is that the power stage driving the motor contains a large deadzone, where small command signals are suppressed by the V_{BE} voltages of the input transistors. During operation, this manifests itself when the cart reaches the endpoint of the track: the cart comes to a stop, then the

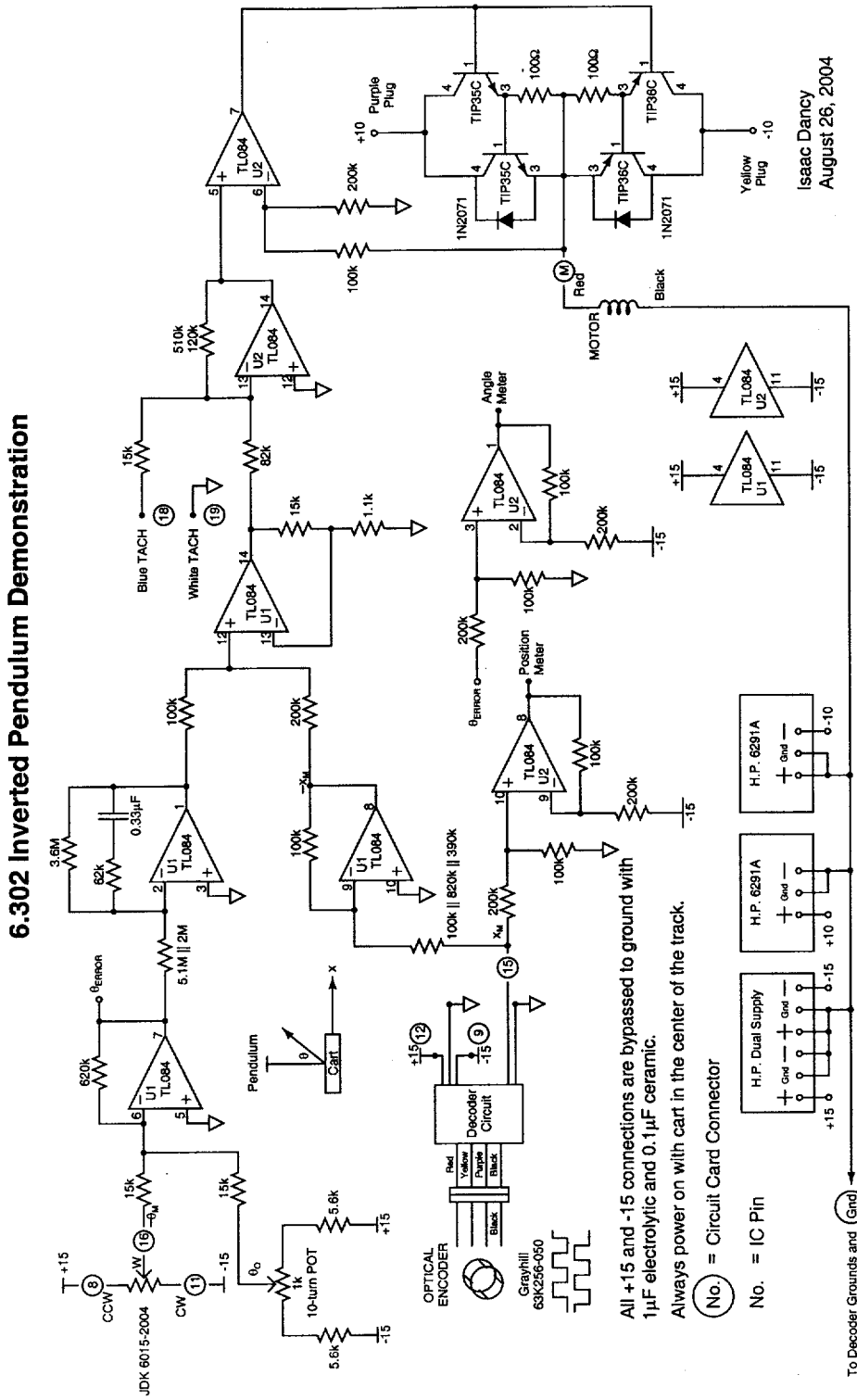

Figure 4-15. Pendulum controller circuit. System eliminates the external 6Ω potentiometer and implements a more straightforward design with two quad J-FET-input operational amplifier circuits, the TL084. Two analog voltmeters display the current measures of angle and position.

pendulum falls for a split second until the error voltage is great enough to develop voltage across the motor windings. The new controller modifies the output stage configuration to avoid this issue, but a modified output stage could certainly be built for the old controller without disrupting or disturbing any of the controller's behavior.

The modified pendulum controller, as well as startup instructions, can be found in Appendix E.

4.4 Results

The system was built as described and works for extended periods of time without worry or reservation. Both sensors function properly and have a lifetime suited for longer system demonstrations.

The new pendulum controller finds the equilibrium point in less than five cycles and remains centered and vertical the rest of the time. In many ways it is boring compared to the old controller which quickly limit cycles and oscillates indefinitely in a quasi-angle-stable manner. In the case that the new controller is deemed too boring and the old controller is used, the former system still behaves better than ever with its sensory improvements and recent modifications.

4.5 Future Work

While the new pendulum controller does work, the behavior of the system at present is not perfectly ideal for demonstrations. The positive feedback around position is perhaps too suppressed, as the controller does not visibly tow-in the pendulum at the endpoints. Furthermore, the motor is a little "soft," as it cannot recover from the same magnitude disturbances that the previous pendulum controller could.

Future work with the pendulum should focus on fine tuning the pendulum controller such that it behaves more similarly to the old system with regard to disturbance and motor performance, while still retaining the superior stability and design of the current new controller.

4.6 Conclusions

Many systems can be made to work temporarily or marginally, but often times the "correct" solution is the only way to ensure durability and robustness for great lengths of time. The previous inverted pendulum system worked well for many years, but ultimately the incorrect sensor choices eventually required a re-evaluation. The only way to truly solve a complex system such as the inverted pendulum is to use components specifically meant for the application from the very beginning.

Furthermore, the importance of documentation cannot be underestimated when it comes to projects of this magnitude. The previous pendulum system did not describe any of its functionality, or even why certain decisions were made regarding component selection. It leaves outsiders left wondering whether the original designer was a genious, or the luckiest engineer of all time. A great design can be limited by poor documentation, which may be the case here — unless, of course, it was a strategic defensive play to mask the controller's confusing behavior.

The new system is well documented and well described. It is the author's hope that the legacy of the inverted pendulum can now endure the test of several more decades at MIT, without incurring the same amount of staff-related stress, sleepless nights, and general confusion that the previous manifestation wrought on many an occasion.

Appendix A

Weblab Assignment

This assignment was written by the author for the web-based laboratory developed in Chapter 2. It makes use of the weblab, as well as the pole-zero applet in Appendix B.

MASSACHUSETTS INSTITUTE OF TECHNOLOGY

Department of Electrical Engineering and Computer Science

6.302 Feedback Systems

Fall 2004 — Issued : September 17, 2004

Filter Blocks WebLab — Due : Friday, September 24, 2004

Introduction

The purpose of this lab is to further examine and explore the response of a real canonical second-order system in terms of its system parameters ζ and ω_n. However, in lieu of going into lab and building many different systems, you will use a web applet to make your measurements. The web applet communicates with a server which controls a single circuit in lab. Throughout the course of this lab you will learn more about the inner-workings of this system.

Be warned: The server manages the queue of job requests, so don't wait until the "night before" to make your measurements unless you are prepared to wait your turn!

Pre-Lab Calculations

1. Consider the following system:

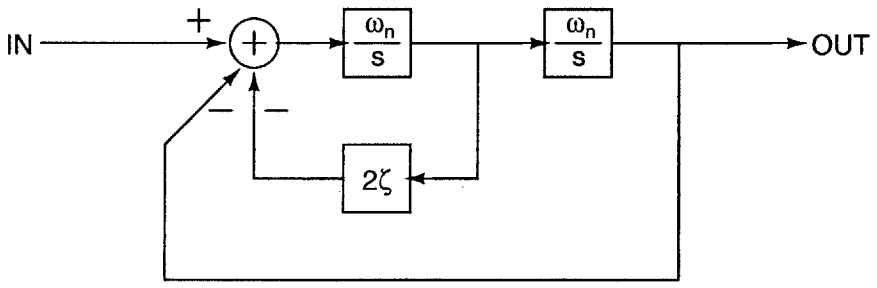

What is the closed-loop transfer function of this system? Have you seen this transfer function before? What does the closed-form of this feedback system

implement?

2. Now suppose that we cascade two copies of this system and have the freedom to control the parameters ζ and ω_n for each system. For each of the following pole-zero plots specify the parameters ζ_1, ζ_2, ω_{n1} and ω_{n2} which will generate a closed-loop transfer function with the corresponding pole-zero plot. (Note: Multiple solutions may exist. Limit $\zeta \leq 1.9$ and $2\pi \cdot 100$ rad/s $\leq \omega_n \leq 2\pi \cdot 10^4$ rad/s.)

(a) Four concurrent poles at $s = -2\pi \cdot 10^3$ rad/s.

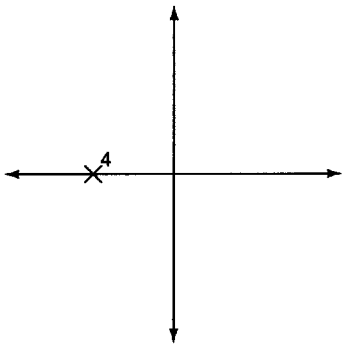

(b) Four poles on the negative real axis.

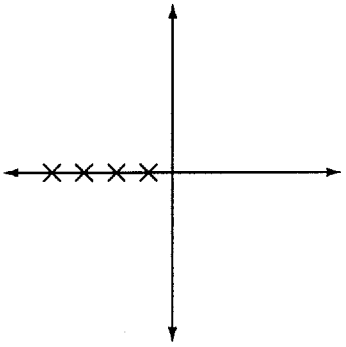

(c) Two conjugate pairs of poles with $\zeta \leq 0.15$ for each system.

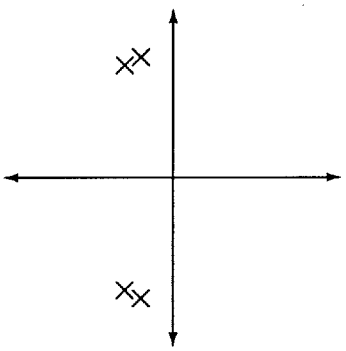

(d) 4th-Order Butterworth filter. All poles a distance $2\pi \cdot 10^3$ rad/s from origin.

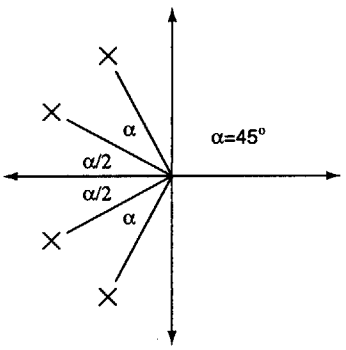

3. Use MATLAB to generate the corresponding Bode plot and step response for each system in Problem 2.

(MATLAB Hint: Use the `subplot` command to put multiple responses on one page.)

4. Figure A-1 is a simplified block diagram of the circuit running at the server of this lab. It uses voltage inputs $AO_0 \rightarrow AO_3$ and multiplier chips (Analog Devices' AD532J) to enable you to tune the closed-loop response to match specific values of ζ and ω_n.

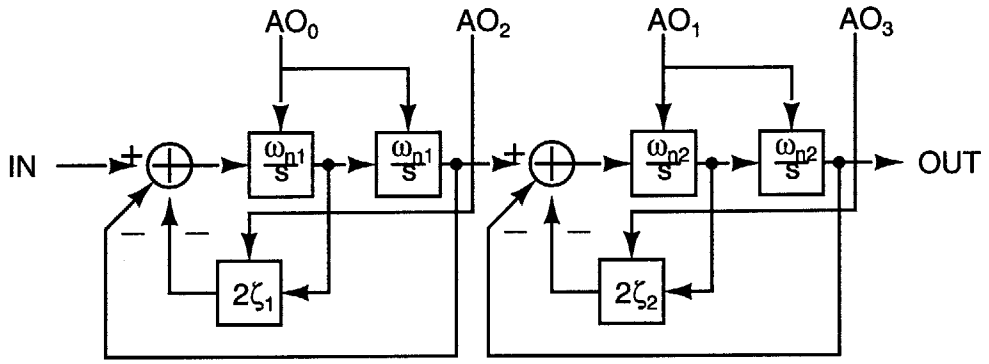

Figure A-1: Simplified block diagram of weblab circuit.

Figure A-2 is the actual circuit, shown here at half size – inputs $AO_{0,2}$ for the first system correspond to inputs $AO_{1,3}$ for the second system. Generate a block diagram for this circuit (in the general form of Figure A-1) and determine the following relationships. (Assume the OP27 is ideal and the AD532J performs a $Z = \frac{A \times B}{10}$ function on two input voltages.)

(a) AO_0 and ω_{n1}

(b) AO_1 and ω_{n2}

(c) AO_2 and ζ_1

(d) AO_3 and ζ_2

5. Parts (a)-(d). Calculate the input voltages that will result in a system that matches your solutions to Problem 2, parts (a)-(d). Note that the input voltages are constrained to $0 < AO_n \leq 5$ V.

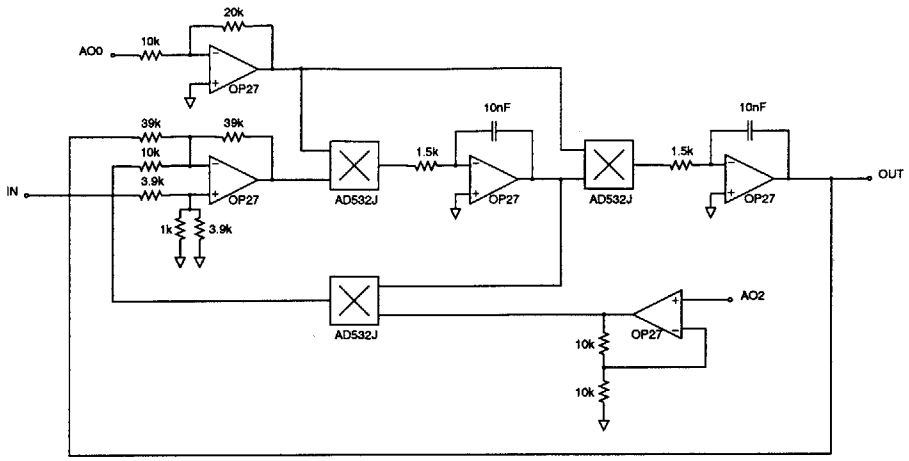

Figure A-2: Actual circuit.

Measurements

You are now ready to go into lab. Log in at `http://i-lab.mit.edu` and click the "Launch Client" button to begin the lab.

1. Run a frequency sweep for each set of voltages in Problem 5 of the prelab. Sweep between 2 and 3 decades in frequency, insuring that you measure all vital parts of the response while keeping your server request manageable. After each sweep make sure you download the data.

   It is possible that some valid combinations for the prelab actually saturate the circuit in this part. You **will** know if this has happened, and should reduce the magnitude peaking of your solution until it no longer saturates the server circuit.

2. Use MATLAB to plot and print out your measured responses. Ambitious students can include the theoretical response on the same plots.

   (MATLAB Hint: This can be achieved by using the form of the `bode` command that returns magnitude, phase and frequency information. Use the `db` command so that the theoretical magnitude data matches the downloaded data.)

3. Butterworth filters are systems that exhibit no magnitude peaking and roll off with some slope depending on the order of the filter. Generate a plot in MATLAB

that compares the magnitude response of systems (a) and (d). What do you notice?

4. **Optional.** Use the pole-zero applet at `http://web.mit.edu/6.302/pz/` to find a pole-zero plot of a third-order Butterworth filter using system (d) as a guide. Do your best to simulate this system with the circuit in lab and print out a plot comparing your measurement with the theoretical response of the ideal third-order Butterworth filter. Make sure you turn in the result of your pole-zero applet efforts.

Write Up

The write up for this lab should be short, simple and informal. Do your best to conserve paper when printing from MATLAB, but do avoid cluttering any one plot excessively.

Appendix B

Pole-Zero Java Applet Assignment

The java applet at `http://web.mit.edu/6.302/www/pz/` written by Brian Williams provides real-time Bode, Nyquist, Nichols and step-response plots [17]. This is a useful tool in understanding the dynamics of linear systems, and therefore the author has written an individual assignment which makes use of the applet extensively. Furthermore, the web-based laboratory in Appendix A references this applet.

MASSACHUSETTS INSTITUTE OF TECHNOLOGY

Department of Electrical Engineering and Computer Science

6.302 Feedback Systems

Fall 2004 Issued : September 17, 2004

Pole-Zero Maps, Bode Plots, and Step Responses Due : Friday, September 24, 2004

Introduction

The purpose of this assignment is to review and refamiliarize yourself with basic pole-zero transfer functions, and the associated Bode plots and step responses which correspond to particular functions and their pole-zero maps.

You will use a Java applet at `http://web.mit.edu/6.302/www/pz/` to do this in a more interactive and enjoyable way. Be prepared to answer questions as you go along and you will have to print out a few screenshots to hand in as well. Each student should do this assignment individually.

Exercises

1. Open the applet and familiarize yourself with the tool. The upper-left portion is an interactive pole-zero map which allows you create systems in real time. The buttons in the upper-right allow you to customize the system. Spend a few minutes to become proficient with all the buttons and the pole-zero map.

   The lower portion of the applet is a series of plots which correspond to the system created in the pole-zero map. The Nichols and Nyquist plots will be introduced later in the term and 6.302 encourages you to regularly return to this applet when you think it would be helpful. The assignment will focus on the Bode plot and step responses.

   Now clear the pole-zero map and add a pole to the negative real axis at $s = -5$ and select the "Bode Plot" tab. What is the corner frequency of this low-

pass filter? How does the magnitude response differ from the corresponding asymptotic Bode plot for this system?

2. Reset and now add a pole at $s = -5 + 5j$. Why does the applet automatically add another pole at $s = -5 - 5j$?

   Drag the conjugate poles horizontally while keeping the x coordinate negative and the y coordinate approximately equal to 5. Does the corner frequency of the system change? What do you notice in the transition of the phase as $x \to 0$? How is this mirrored in the magnitude response?

   Now look at the step response and put one pole at $s = -5$. Drag that pole vertically while maintaining the x coordinate. What happens to the step response?

3. Reset and add many poles in one location of the negative-real axis and note the effect in step response. Does the rise time or final value change? What system element does this simulate?

4. Many times throughout feedback design you will encounter a system with singularities at undesirable locations. It is often tempting to negate these singularities by cancelling them out. That may not always be a wise decision.

   Create many poles along the negative-real axis in a linear fashion. You should have about 8-10 poles spread evenly in the end. Now, suppose you really wanted a system to respond like a system with the transfer function $\frac{1}{0.1s+1}$, and decide to cancel all the poles with a zero with the exception of the pole at $s = -10$. Do this but don't take measures to line up all the cancellations exactly. What features do you notice in the step response and Bode plot that differ from the desired response?

5. Create a system with one pole and one zero. Drag each along the real-axis and note how each singularity affects the step response.

   For each combination you should first predict the initial and final values using

the Initial Value and Final Value Theorems then test your solution with the applet.

(a)

$$\frac{0.2s+1}{0.125s+1}$$

(b)

$$\frac{0.125s+1}{0.2s+1}$$

(c)

$$\frac{0.2s+1}{1-0.2s}$$

(d)

$$\frac{1-0.2s}{0.2s+1}$$

Pick one and print it out. Find some creative way to demonstrate your handy work. *Hint.* You can enter the command `whoami` into a terminal and have that present during the screen capture.

6. Later in the course we will cover series compensation, which is basically a way to alter the open-loop characteristics of a transfer function to improve its behavior in a closed-loop sense. Some basic things we'll want to do is improve the low-frequency gain while decreasing the high-frequency gain, or making the phase more positive at a particular frequency. We can do that by adding a system – consisting of a pole and a zero – to the system we are compensating.

   Create a pole-zero system with the pole at a lower frequency, keeping both negative and real. How does the high-frequency gain change as the singularities are spread further apart? How does the phase minimum change at the same time?

Now create a pole-zero system but keep the zero at a lower frequency. What is the maximum phase "bump" you can generate withing the limits of the applet? What is the ratio of the pole-zero locations at this maximum?

Many times this ratio is limited to 10 due to limitations of real-world systems. Make the ratio of your system 10 and note the Bode plot at different combinations of pole-zero location while maintaining the ratio of 10. Doe the phase bump differ between combinations?

The systems in this part are known as lag and lead compensators, and will be covered and used later in 6.302.

Appendix C

Magnetic Levitation Assignment

This assignment was written by Dr. Kent Lundberg for an in-class project for 6.302 Feedback Systems which debuted during the Fall 2003 semester. Students were given the kits described in [12, 13] and the project was an overwhelming success, highlighted by a student's levitation project appearing on the front page of the school newspaper during the final week of classes. See Chapter 3 for a description of how to complete this assignment and how to make the levitation kits even cheaper.

MASSACHUSETTS INSTITUTE OF TECHNOLOGY

Department of Electrical Engineering and Computer Science

6.302 Feedback Systems

Fall Term 2003 — Issued : November 12, 2003

Lab 3 Maglev Project — Due : Friday, December 5, 2003

The purpose of this lab is to build and improve a small magnetic levitation (maglev) system. You will be given a kit to build the basic system (which you can keep after checkoff). After building the basic system, you will evaluate the dynamics of the system and design a compensator for it. You are encouraged to also improve other aspects of the system, such as the sensor, the electromagnet, the electronics, and the levitated object. This lab is an open-ended design project, so be creative!

Basic System Construction

The structural features of the basic maglev system are shown in Figure 1. The schematic of the drive electronics is shown in Figure 2. The kit you will receive includes all of the parts shown in the schematic (and listed in Figure 3), but does not include the wooden stand or the object for levitation (you will have to provide your own). For this lab, you will need to build the basic system as shown in the figures.

This kit is based on a low-cost design developed by Guy Marsden [18]. In the basic system, the position of the levitated object is sensed by the SS495 Hall-effect sensor. The output voltage of the sensor drives the input of the MIC502 fan-management chip. The fan-management chip produces a pulse-width modulated (PWM) drive signal to the LMD18201 H-bridge chip. This PWM signal adjusts the average current in the solenoid, which controls the magnetic field.

Please use care in the construction of your system. Read the data sheets for each IC in the schematic to familiarize yourself with the behavior and operation of the circuit. While the EECS Department and National Semiconductor have been

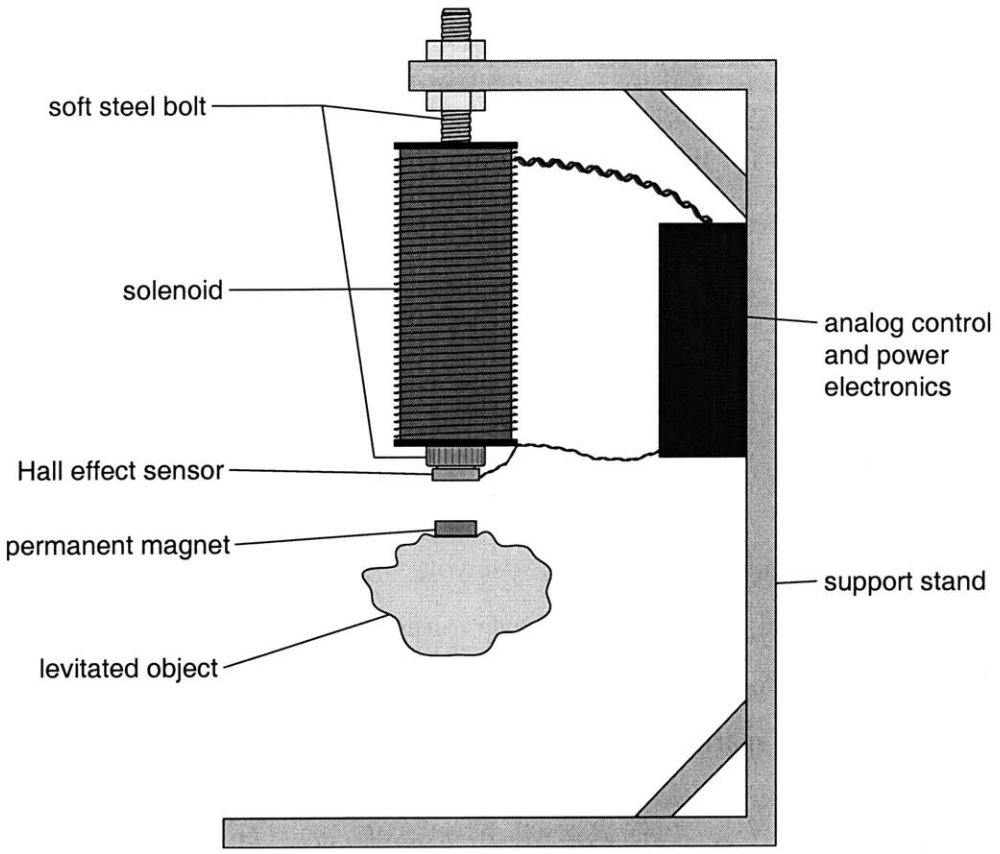

Figure 1: An assembled magnetic levitation system

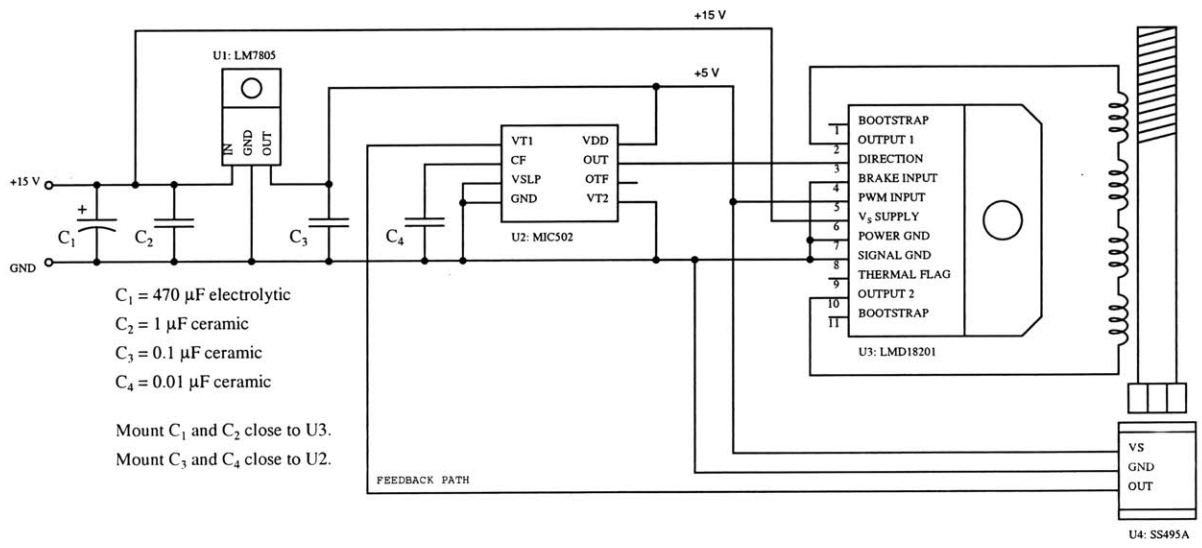

Figure 2: Schematic of magnetic levitation system

U1	LM7805	voltage regulator
U2	MIC502	fan-management IC
U3	LMD18201	motor H-bridge IC
U4	SS495A	Hall-effect sensor
C1	470 μF	electrolytic capacitor
C2	1 μF	ceramic capacitor
C3	0.1 μF	ceramic capacitor
C4	0.01 μF	ceramic capacitor
	prewound solenoid	
	soft-steel carriage bolt	
	neodymium magnets (2)	
	heatsink for LMD18201	
	small circuit board	

Figure 3: List of kit contents

generous in making these kits available to you, we cannot afford to donate large numbers of parts to you. We will expect every student who receives a kit to complete the lab. While we will be tolerant of reasonable but destructive errors, we have only a very small supply of spares. Build carefully!

Testing

For the basic system to work, the polarities of the solenoid, the sensor, and the magnet must all be correct. When correct, you should notice that the solenoid repels the magnet when the magnet is too close. You may have to experiment with the polarity of the solenoid winding, the placement of the sensor, and the orientation of the magnet.

An ammeter can assist in verifying correct operation. The input current should be large (up to 0.5 A) if the magnet is too far from or too close to the solenoid. At the operating point, the current consumption for this kit is around 100 mA.

The correct behavior is also very sensitive to the weight of the levitated object. The actual lifting capability of the basic system is very small (about half-a-pencil with the magnet). Be prepared to experiment.

Compensation

Evaluate the dynamics of the system and design a compensator for it. To evaluate the transient behavior of the improved system, you will need to modify the circuit to provide an input signal, as shown in Figure 4. Measure the step response of the system to small input steps.

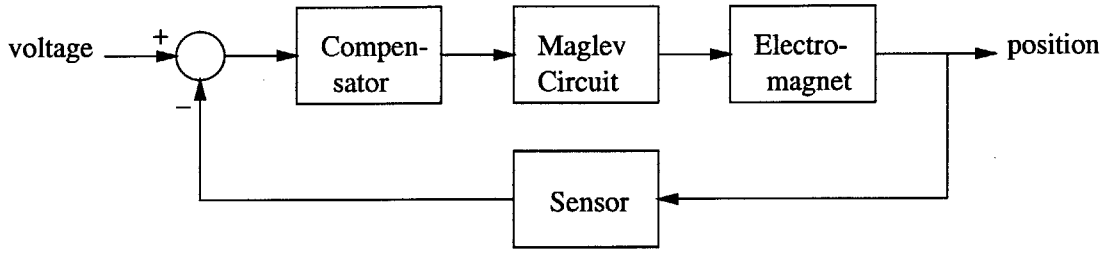

Figure 4: Block diagram of modified magnetic levitation system

Due to the PWM drive to the electromagnet, the output of the sensor may include a lot of ripple. You may wish to filter out this ripple with a low-pass filter before the oscilloscope. Note that this filter does not go inside the feedback loop (for obvious reasons), but goes between the sensor output and the scope.

Design a simple dominant-pole, lag, or lead compensator to stabilize the system and improve the transient response. Design for a peak overshoot of less than 20% in the step response.

Modifications

You are encouraged to improve other aspects of the system. Modifications to consider include sensor selection and placement, the electromagnet size and design, the characteristics of the levitated object, and the design of the power electronics.

For example, one aspect of the design which can be improved is the position sensor. The Hall-effect sensor detects the strength of the magnetic field produced by the magnet on the levitated object. However, because the Hall-effect sensor is directly below the electromagnet, its output will depend not only on the the distance between the sensor and the permanent magnet but also on the strength of magnetic field generated by the solenoid.

The large maglev system analyzed in lecture uses a photo-detector to sense position [19, 20]. In this approach, the steel ball levitates between a collimated light source and the photo-detector to produce a shadow, as shown in Figure 5. This sensor scheme is simple and reliable and can produce a close-to-linear estimation of position. However, it requires careful alignment and additional parts, including a light bulb or LED, a photo-detector (CdS cell), focusing optics, and assorted electronics.

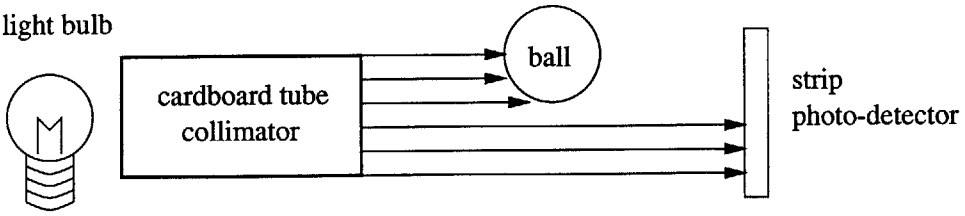

Figure 5: Diagram of simple light sensor system

Lab Report

Write a report that completely documents your design. In particular,

1. Describe your efforts to evaluate, characterize, and model the basic system. Provide bode plots and transfer functions, if appropriate.

2. Document all changes that you made to the basic system, such as sensor type and location, the electromagnet coil design, the type of levitated object, the power electronics, and (of course) the compensator.

3. Provide complete schematics of any circuitry that you changed in or added to the basic design and describe its function.

4. Describe the behavior of your improved system. Provide step responses, bode plots, and transfer functions.

5. Include references to any books, articles, datasheets, or web sites that you used in your research and design.

Your report should be complete, detailed, and neat. Using your report, a reasonable technician should be able to recreate your design and results.

Contest

At checkoff, you must demonstrate your improved system to the TAs. A number of system characteristics will be tested and evaluated. Prizes will be awarded for the best designs in the following categories:

Best Transient Response	20 extra credit points
Widest Dynamic Range	20 extra credit points
Best Disturbance Rejection	20 extra credit points
Heaviest Object Lifted	10 extra credit points
Lowest Power Consumption	10 extra credit points
Most Artistic System	Tosci's gift certificate

All entrants must be ready for checkoff starting at 4pm on December 5. Lab reports must be complete at this time. Late entrants will be disqualified.

1. **Widest Dynamic Range:** Largest periodic movement of the object, measured with a ruler, for a square-wave or sine-wave input.
2. **Best Disturbance Rejection:** Largest ratio between heaviest object levitated to lightest object levitated, using the same number of magnets.
3. **Heaviest Object Lifted:** Weight of object, maximum of one magnet.
4. **Lowest Power Consumption:** Measured with ammeter on the single 15-V supply.
5. **Most Artistic System:** Beauty is in the eye of the beholder.

Each student may enter up to two categories. Decisions of the judges are final, and may be arbitrary.

Acknowledgements

Special thanks to National Semiconductor for a generous donation of LMD18201s.

Appendix D

New Inverted Pendulum Schematic and Power-Up Procedure

This appendix reviews the new inverted pendulum controller and optical encoder schematics from Chapter 4 and explains how to run it as an in-class demonstration. This controller will be referred to as the "6.302 Inverted Pendulum Controller" given it utilizes a 6.302 inverted pendulum lecture to design the control scheme.

See Appendix E to see similar information concerning the previous inverted pendulum demonstration.

6.302 Inverted Pendulum Demonstration

Read all steps before attempting to power on the inverted pendulum demonstration.

1. Make all system connections indicated in the circuit schematic. Before making power connections, first check that each supply is set to the proper voltage. The current capability of the ± 10 V supplies does not need to exceed 1 A.

2. Move cart to the center of the track and power on the ± 15 V supplies. The position meter should read 7.5 V.

3. Observe that by swinging the pendulum the angle meter should either saturate at $+15$ V or 0 V. Hold the pendulum to the right while turning on the -10 V supply.

4. Slowly rotate the pendulum to the vertical position without overcompensating. When the angle voltmeter reads close to 7.5 V, turn on the $+10$ V supply.

5. Hold the pendulum through to the end of the initial oscillation and release the pendulum once the system has settled.

6. If the cart does not use the track evenly and offsets to one side, the possible reasons are that the supplies are not perfectly symmetric or a misalignment has developed in the pendulum or controller. If the pendulum runs off the right side of the track, or is generally offset to the right, trim the controller potentiometer counter-clockwise, and vice versa. Use small increments.

The system is now configured and is capable of running for several hours.

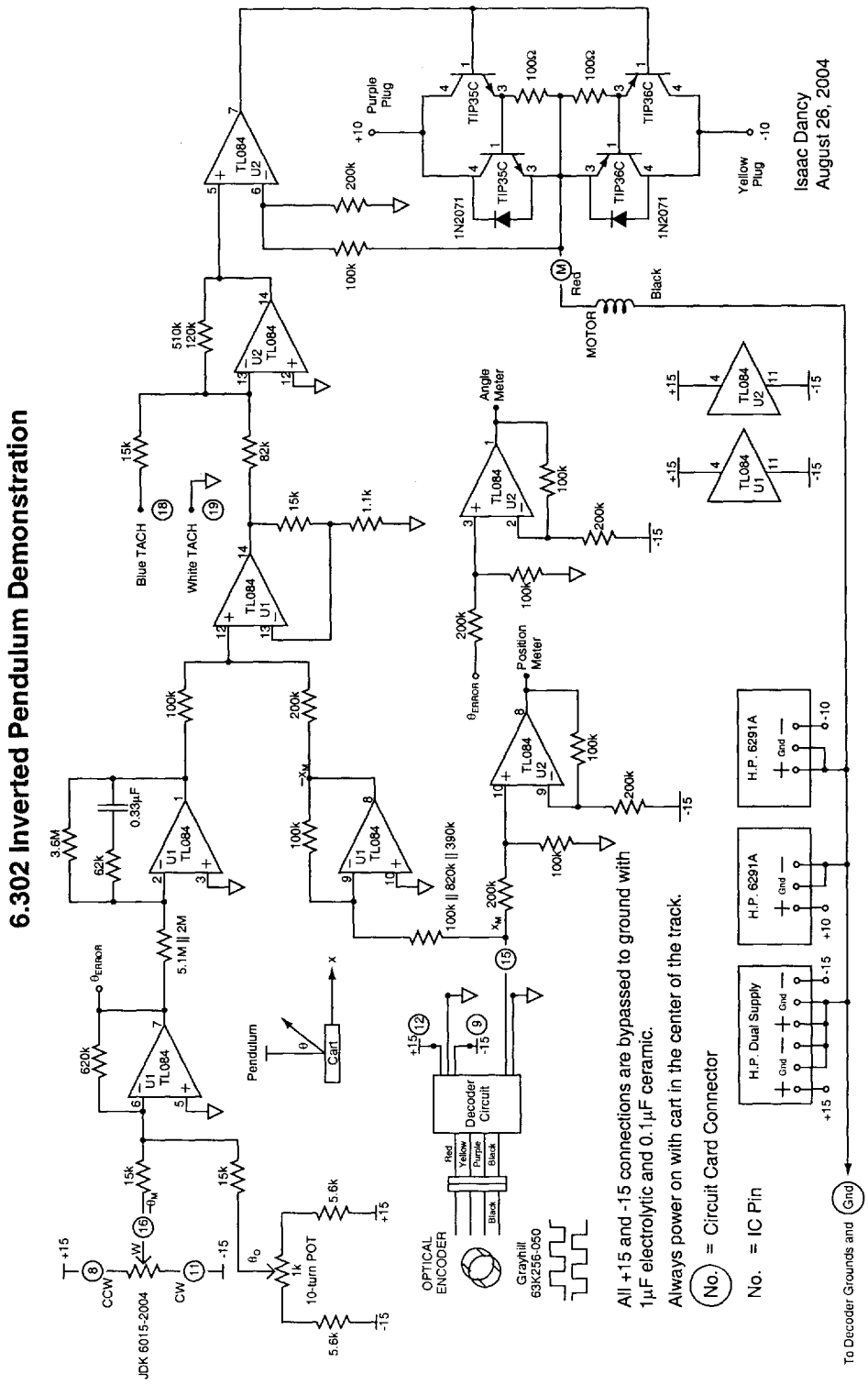

Figure D-1: 6.302 Inverted Pendulum Schematic

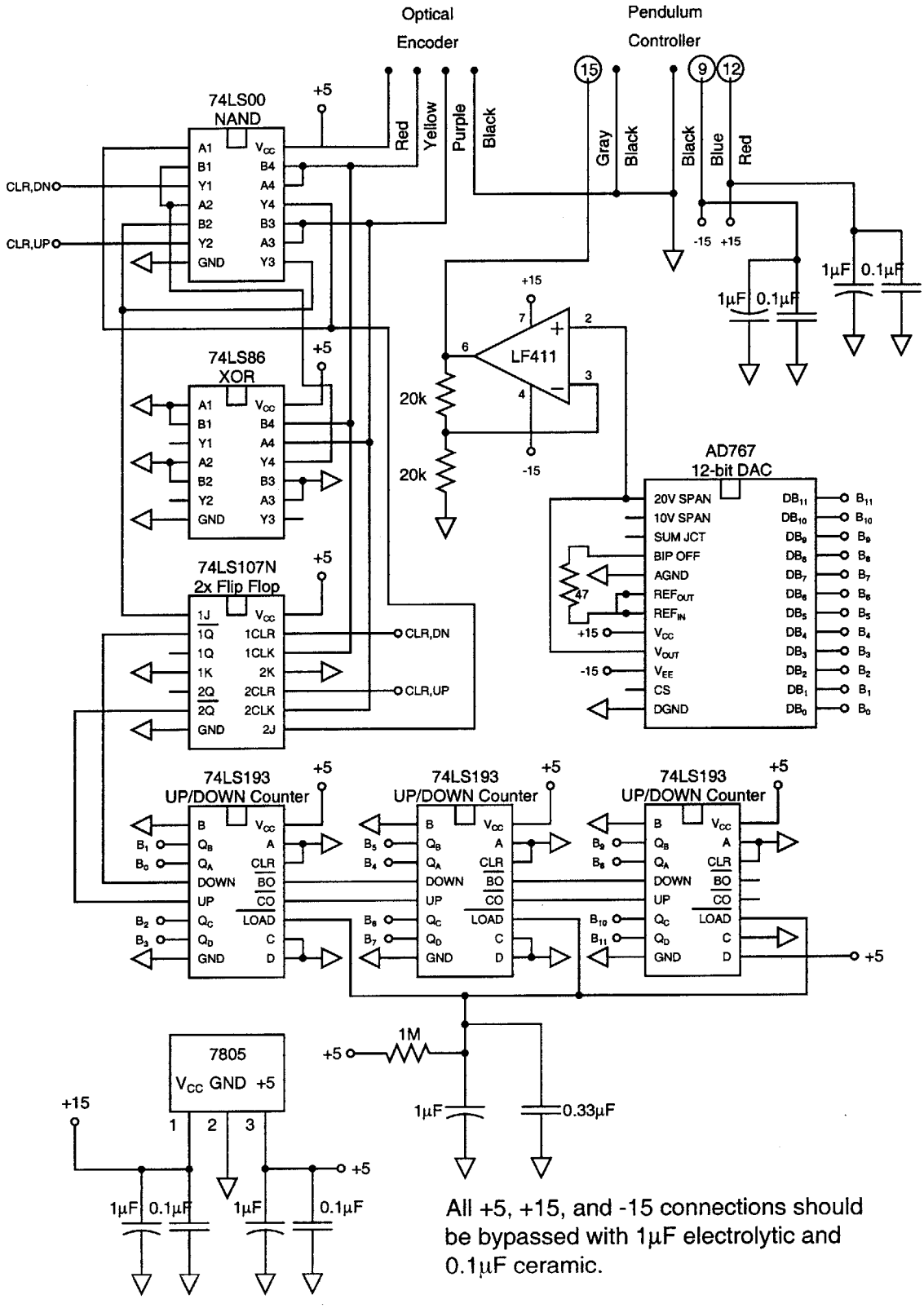

Figure D-2: Decoder Schematic

Appendix E

Former Inverted Pendulum Schematic and Power-Up Procedure

This appendix reveals the former inverted pendulum controller and steps through how to run the inverted pendulum system with it. The schematic has been very slightly modified in order to maintain compatibility with new sensor implementations. This controller is sometimes referred to as the "6.003 Inverted Pendulum Controller" given this title appears on the old, handwritten schematic.

Any knowledge of who built this demonstration has long since passed into oral tradition — this author could certainly not find any names or claims of authorship while analyzing the system other than the markings *FBB14* found on the cart — otherwise authorship credit would be mentioned here. See Chaper 4 for details about the inverted pendulum system model and the development of a new, more cognizant and understood system controller.

6.003 Inverted Pendulum Demonstration

Read all steps before attempting to power on the inverted pendulum demonstration.

1. Make all system connections indicated in the circuit schematic. Ensure that the 6Ω potentiometer is set completely counter-clockwise.

2. Make sure the "Loop Gain" potentiometer is in the 12 O'Clock position, then power on all the power supplies while holding the pendulum vertically at the center of the track. Sequential power on is adequate. Check that all supplies are at the correct settings before power on.

3. If the controller angle sense is not tuned correctly, the cart will not rest directly below the held pendulum. Turn the potentiometer labelled "θ_0" clockwise to move the cart to the right, and turn the potentiometer counter-clockwise to move the cart to the left.

4. Once the cart is directly below the pendulum, release the pendulum. If the position sense is not correct the pendulum will not oscillate around the center of the track. (*Warning.* The cart may drive off the end of the track if severely misadjusted, so you must be prepared to catch the pendulum during this step.) Turn the potentiometer labelled "x_0" clockwise if the system is offset to the right, and turn the potentiometer counter-clockwise if the system is offset to the left. This adjustment is very sensitive, so make small adjustments.

5. Once the system oscillates around the center of the track, adjust the loop gain to achieve the desired performance. Turn the potentiometer labelled "Loop Gain" clockwise for faster movement, and turn the potentiometer counter-clockwise for slower movement. Additionally, clockwise adjustment will decrease the amount of track the cart uses, while counter-clockwise adjustment will increase the amount of track.

The system is now configured and is capable of running for several hours.

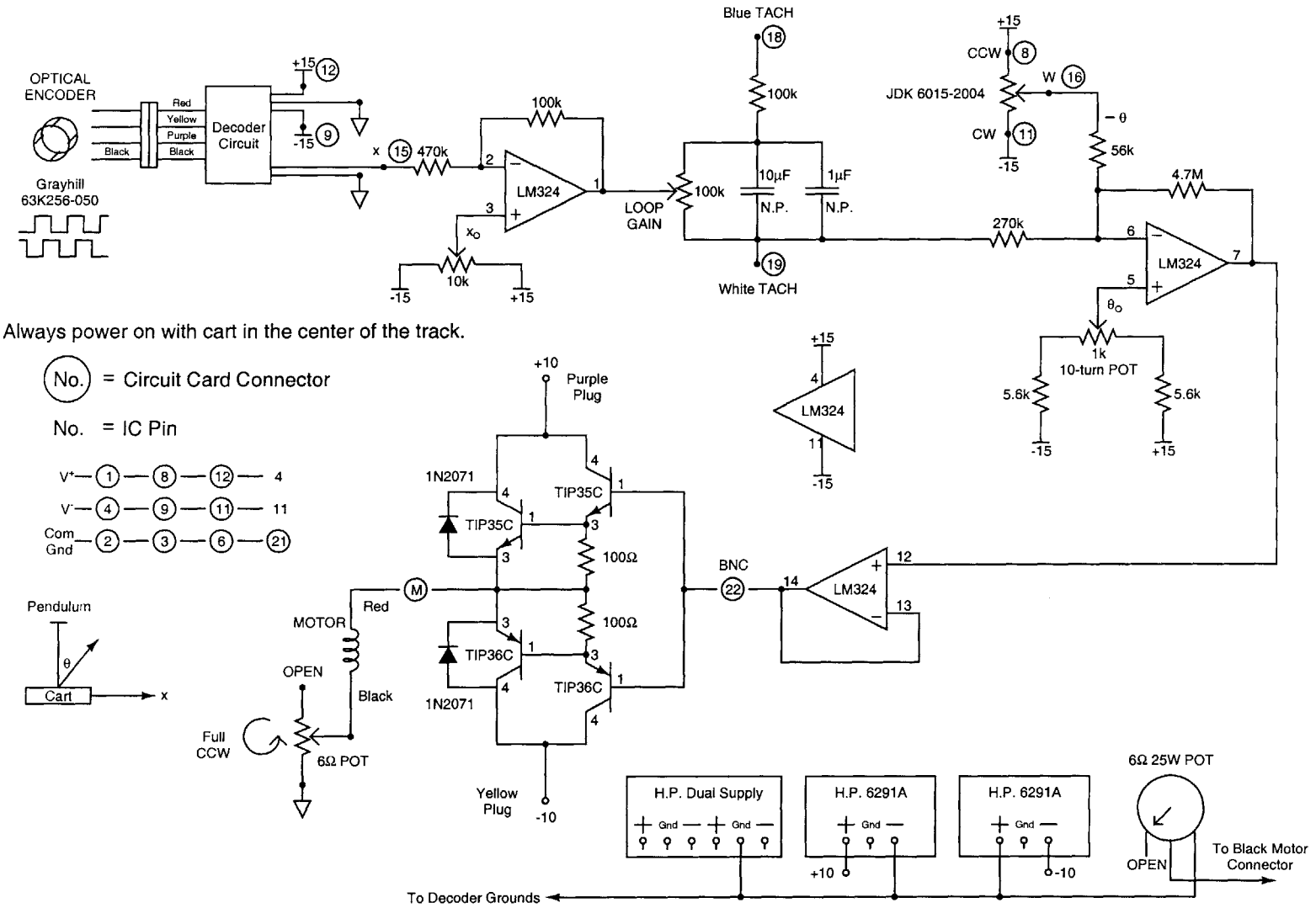

Figure E-1: 6.003 Inverted Pendulum Schematic

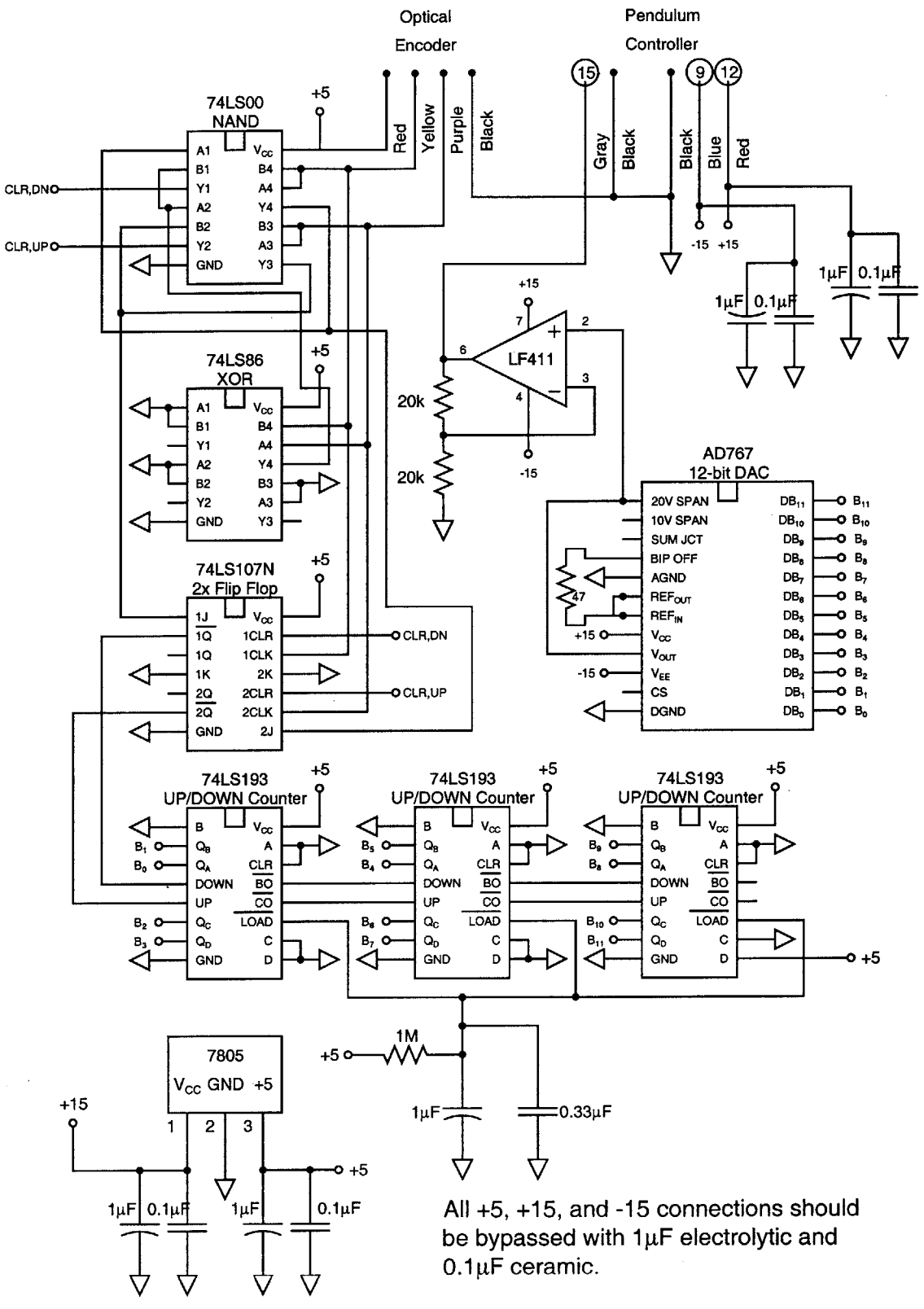

Figure E-2: Decoder Schematic

References

[1] Analog Devices, "OP27: Low-noise, precision operational amplifier," Datasheet, Jan. 2003.

[2] ——, "OP37: Low noise, precision, high speed operational amplifier ($A_{VCL} \geq 5$)," Datasheet, Dec. 2002.

[3] G. V. Núñez, "Design and implementation of a feedback systems web laboratory prototype," Advanced Undergraduate Project, Massachusetts Institute of Technology, Department of Electrical Engineering and Computer Science, May 2004.

[4] S. Lokanathan, "Extension to the feedback systems web laboratory client prototype," Advanced Undergraduate Project, Massachusetts Institute of Technology, Department of Electrical Engineering and Computer Science, July 2004.

[5] B. A. Hutchins, *Builder's Guide and Preferred Circuits Collection.* Ithaca: Electronotes, 1986.

[6] H. Chamberlin, *Musical Applications of Microproccessors*, 2nd ed. Indianapolis: Hayden Books, 1985.

[7] J. Harward *et al.*, "iLab: A scalable architecture for sharing online experiments," In *International Conference on Engineering Education*, Oct. 2004.

[8] LabJack Corporation, "LabJack — USB-based data acquisition and control," `http://www.labjack.com`.

[9] R. Johnson, "Programmable state-variable filter design for a feedback systems web-based laboratory," Advanced Undergraduate Project, Massachusetts Institute of Technology, Department of Electrical Engineering and Computer Science, Feb. 2004.

[10] Digi-Key Corporation, `http://www.digikey.com`.

[11] G. V. Núñez, I. J. Dancy, and K. H. Lundberg, "A web-based linear-systems iLab," Submitted to *American Control Conference*, Gainesville, FL, 2005.

[12] K. A. Lilienkamp and K. H. Lundberg, "Low-cost magnetic levitation project kits for teaching feedback system design," in *American Control Conference*, Boston, MA, June 2004, pp. 1308–1313.

[13] K. H. Lundberg, K. A. Lilienkamp, and G. Marsden, "Low-cost magnetic levitation project kits," *IEEE Control Systems Magazine*, vol. 24, no. 5, Oct. 2004.

[14] W. G. Hurley, M. Hynes, and W. H. Wölfle, "PWM control of a magnetic suspension system," *IEEE Transactions on Education*, vol. 47, no. 2, pp. 165–173, May 2004.

[15] K. A. Lilienkamp, personal communication, 2003.

[16] J. Shafran, personal communication, 2004.

[17] B. Williams, "Educational java applet for linear system responses," Advanced Undergraduate Project, Massachusetts Institute of Technology, Department of Electrical Engineering and Computer Science, May 2004.

[18] G. Marsden, "Levitation!" *Nuts and Volts Magazine*, vol. 24, no. 9, pp. 58–61, Sept. 2003.

[19] H. Woodson and J. Melcher, *Electromechanical Dynamics — Part I.* New York: Wiley, 1968.

[20] J. Roberge, *Operational Amplifiers: Theory and Practice.* New York: Wiley, 1975.